Dynamic Decode-and-Forward based Cooperative NOMA with Spatially Random Users

Yong Zhou, *Member, IEEE*, Vincent W.S. Wong, *Fellow, IEEE*, and Robert Schober, *Fellow, IEEE*

***Abstract*—Non-orthogonal multiple access (NOMA) is a promising spectrally-efficient multiple access technique for the fifth generation (5G) wireless networks. In this paper, we propose a dynamic decode-and-forward (DDF) based cooperative NOMA scheme for downlink transmission with spatially random users. In DDF-based cooperative NOMA, the base station transmits the superposition of the signals intended for the paired NOMA users. The user closer to the base station forwards the signal intended for the far user as soon as it can successfully decode its own signal and the signal intended for the far user. We consider two user pairing strategies, namely random and distance-based user pairing, which require one-bit feedback and the users' distance information, respectively. For each user pairing strategy, we derive the outage probability of the proposed NOMA scheme by using tools from stochastic geometry. Furthermore, based on the obtained outage probability, we derive the diversity order and the sum rate of the paired NOMA users. Simulation results validate the analytical results and demonstrate that the proposed DDF-based cooperative NOMA scheme achieves a lower outage probability and a higher sum rate than orthogonal multiple access (OMA), conventional NOMA, and cooperative NOMA.**

***Index Terms*—Non-orthogonal multiple access, dynamic decode-and-forward, user pairing, spatially random users.**

I. Introduction

Non-orthogonal multiple access (NOMA) is a spectrally-efficient multiple access technique, which has the potential to meet the exponentially increasing traffic demand and to support massive connectivity for billions of devices in fifth generation (5G) wireless networks [2]–[4]. With NOMA, multiple users can be simultaneously served by one base station in the same frequency channel and with the same spreading code by allocating different transmit powers to the users [5]. Compared to orthogonal multiple access (OMA), NOMA enables a more favorable tradeoff between system throughput and fairness for users with diverse channel conditions.

Manuscript received on July 20, 2017; revised on Nov. 25; 2017, accepted on Feb. 13, 2018. This work was supported by the Natural Sciences and Engineering Research Council (NSERC) of Canada. This paper was presented in part at the *IEEE Global Communications Conference (GLOBECOM)*, Singapore, Dec. 2017 [1]. The editor coordinating the review of this paper and approving it for publication was Professor Pierluigi Salvo Rossi.

Y. Zhou was with the Department of Electrical and Computer Engineering, The University of British Columbia, Vancouver, Canada. He is now with the School of Information Science and Technology, ShanghaiTech University, Shanghai, China (e-mail: zhou@ece.ubc.ca).

V. W.S. Wong is with the Department of Electrical and Computer Engineering, The University of British Columbia, Vancouver, BC, Canada, V6T 1Z4 (e-mail: vincentw@ece.ubc.ca).

R. Schober is with the Institute for Digital Communications, Friedrich-Alexander University of Erlangen-Nuremberg, Germany (e-mail: robert.schober@fau.de).

Color versions of one or more of the figures in this paper are available online at http://ieeexplore.ieee.org.

NOMA has recently attracted significant research interest [6]–[14]. In particular, the authors in [6] evaluate the system level performance of downlink NOMA transmission, demonstrating the importance of transmit power allocation and user pairing for the design of efficient NOMA systems. The author in [7] proposes an optimal transmit power allocation scheme to maximize the sum rate of two paired users in multiple-input multiple-output (MIMO) NOMA systems when either instantaneous or statistical channel state information (CSI) is available at the base station. Transmit power allocation for multicarrier NOMA systems is studied in [8], where the paired users are ordered based on their quality of service (QoS) requirements. A joint subcarrier and power allocation policy is developed in [9] to maximize the weighted sum rate of multicarrier NOMA systems, where the base station simultaneously serves the uplink and the downlink users. The application of NOMA in narrowband Internet of Things (IoT) systems is studied in [10], where the number of simultaneously connected IoT devices is maximized. In addition, the impact of user pairing on the outage probability and sum rate of NOMA is investigated in [11], where both fixed and cognitive radio-based power allocation are considered. In [12], signal alignment is utilized to mitigate the co-channel interference between different NOMA user pairs, and the performance of MIMO NOMA systems for both uplink and downlink transmission is analyzed. Random beamforming is employed in [13] to reduce the channel estimation overhead in millimeter-wave NOMA systems and tools from stochastic geometry are utilized to analyze the sum rate of the paired users. However, in the aforementioned studies, by sharing the frequency channel and the transmit power with the near user[1], the performance of the far user can be degraded due to NOMA [15].

Cooperative NOMA can enhance the spectral efficiency by introducing a cooperative diversity gain [16]. Based on the principle of NOMA, successful decoding of the signal intended for the far user is a prerequisite for performing successive interference cancellation (SIC) and decoding at the near user. When the signal intended for the far user is available, the near user can act as a relay and forward the signal to the far user, alleviating the adverse effects of NOMA. The application of simultaneous wireless information and power transfer in cooperative NOMA systems is studied in [17], where the near user forwards the signal to the far user using the energy harvested from the base station. Another category of cooperative NOMA utilizes dedicated relays to facilitate

[1]For two paired NOMA users, we refer to the user closer to the base station as the near user and to the other user as the far user.

cooperative transmission [18]–[20]. In [18], [19], a dedicated decode-and-forward (DF) relay is coordinated by the base station to enhance the reception reliability of cell edge users. The impact of relay selection on the performance of downlink NOMA transmission is investigated in [20], where the direct links between the base station and the users are assumed to be blocked. However, the aforementioned cooperative NOMA schemes require an additional time slot for relay transmission. To address this issue, the authors in [21], [22] analyze the outage probability of full-duplex cooperative NOMA for a two-user scenario, where the near user acts as a full-duplex relay to assist the transmission of the far user. However, full-duplex relaying suffers from a higher hardware implementation complexity compared to half-duplex relaying, and introduces non-negligible self-interference that can degrade the performance of the near user. Moreover, neither user pairing nor random user locations are taken into account in [21], [22].

Dynamic decode-and-forward (DDF) relaying is a physical layer cooperation strategy, which allows a half-duplex relay to provide a cooperative diversity gain without consuming additional time slots [23]. Based on lattice coding/decoding schemes, the authors in [24] propose a DDF relaying scheme which has a low implementation complexity. The authors in [25] characterize the achievable diversity-multiplexing tradeoff (DMT) for DDF relaying and propose a DMT optimal code construction. However, to the best of our knowledge, the application of DDF relaying in NOMA systems with spatially random users has not been studied, yet.

In this paper, we propose a DDF-based cooperative NOMA scheme for downlink transmission. In particular, the base station superimposes the signals intended for two paired NOMA users by allocating different transmit powers to them. The near user decodes both signals based on partial reception, where the reception duration depends on the quality of the channel between the near user and the base station. Subsequently, the near user acts as a relay to improve the channel quality of the far user and to increase the probability that the far user can successfully decode the signal. To model the random user locations, we consider a general network setting, where the spatial locations of the users are modeled as a homogeneous Poisson point process (PPP). For this network scenario, we first investigate the performance of DDF-based cooperative NOMA with *random user pairing*, where the near and the far users are randomly selected for NOMA transmission based on one-bit feedback. Furthermore, to investigate the impact of the spatial locations of the paired users on the network performance, we analyze the performance of DDF-based cooperative NOMA with *distance-based user pairing*, where the near and the far users are ordered based on their distances with respect to the base station before user pairing is performed. The main contributions of this paper are summarized as follows:

- We develop a tractable performance analysis framework for the proposed DDF-based cooperative NOMA scheme for downlink transmission with spatially random users. We consider two user pairing strategies, which entail different CSI requirements and offer different tradeoffs between network performance and implementation complexity.
- Tools from stochastic geometry are utilized to derive the outage probabilities of the near and the far users in the proposed DDF-based cooperative NOMA scheme for the random and distance-based user pairing strategies. Based on the derived outage probability, we obtain the diversity order and the sum rate for both user pairing strategies. Our results reveal that the proposed DDF-based cooperative NOMA scheme can achieve a diversity order of two for the far user without sacrificing spectral efficiency.
- Simulations are used to validate the analytical results. We show that the proposed DDF-based cooperative NOMA scheme outperforms OMA, conventional NOMA, and cooperative NOMA in terms of the outage probability and the sum rate. The sum rate gain of DDF-based cooperative NOMA over OMA is higher when users with more diverse target data rates are paired. Moreover, the performance gain of distance-based user pairing over random user pairing depends on the user density and the target data rate.

Our work differs from the existing works on DDF relaying [23]–[25] in several aspects. First, the proposed scheme exploits the benefits of both DDF relaying and NOMA, to facilitate both cooperative diversity and superimposed transmission. Second, instead of a fixed-topology network, we consider downlink transmission with spatially random users, where the randomness of both the channel fading and the two-dimensional spatial locations of the near and the far users is taken into account. Third, instead of analyzing the asymptotic outage probability or an upper bound on the outage probability, we derive an analytical expression for the approximate outage probability, which is shown to be accurate.

The remainder of this paper is organized as follows. Section II describes the network topology and the signal model for the proposed DDF-based cooperative NOMA scheme. We characterize the outage probability, the diversity order, and the sum rate of the proposed scheme with random and distance-based user pairing strategies in Sections III and IV, respectively. Simulation and analytical results are presented in Section V. Finally, Section VI concludes this paper.

We use the following notations in this paper: $\mathbb{P}(x)$ and $\mathbb{E}_y(\cdot)$ denote the probability of event x and the expectation with respect to random variable y, respectively. The conjugate and the amplitude of a complex variable are denoted as $(\cdot)^*$ and $|\cdot|$, respectively. $\mathbb{1}(\cdot)$ denotes the indicator function. $\min\{x, y\}$ is equal to x if $x \le y$, and equal to y otherwise. $\max\{x, y\}$ is equal to x if $x > y$, and equal to y otherwise.

II. System Model

A. Network Topology

Consider a downlink transmission scenario, which consists of one base station and multiple users, as shown in Fig. 1. Base station S is located at the center of a circular network coverage area with radius R and is equipped with M antennas. The spatial locations of the users are assumed to follow a homogeneous PPP[2], denoted as Φ, with density λ, which

[2]The proposed framework can be generalized to non-homogeneous PPP by first deriving the probability density functions (PDFs) of the user distances based on the corresponding intensity function and then applying them for calculation of the outage probability and the sum rate.

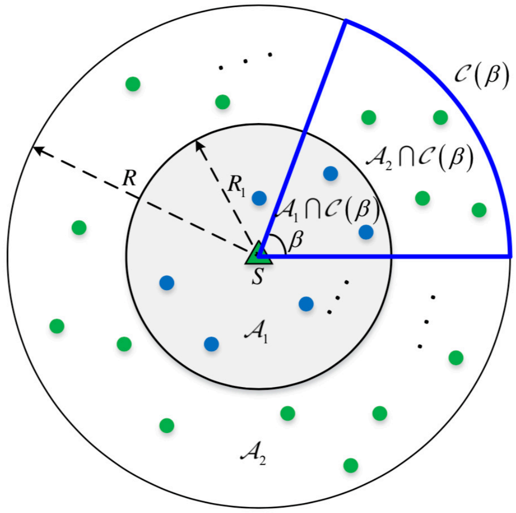

Fig. 1: The network topology for downlink NOMA transmission with spatially random users. The network coverage area is divided into multiple sectors. We focus on a typical sector $\mathcal{C}(\beta)$, where β denotes the angle of the sector. Base station S pairs one user inside $\mathcal{A}_1 \cap \mathcal{C}(\beta)$ and one user inside $\mathcal{A}_2 \cap \mathcal{C}(\beta)$, where $\mathcal{A}_1$ and $\mathcal{A}_2$ are the inner circle and the outer annulus, respectively. The blue and green dots represent the near and the far users, respectively.

represents the average number of users per unit area [26]. Each user has a single antenna. The base station and all users operate in the half-duplex mode. The channel between any two transceivers suffers from path loss and quasi-static Rayleigh fading. The channel fading coefficients are assumed to remain invariant during one time slot and vary independently across different links [11]–[13].

To mitigate the co-channel interference and to reduce the system complexity, we always pair two users by NOMA as in [17]–[22] and adopt hybrid multiple access. In particular, the network coverage area is divided into M sectors and each sector is served by one antenna of the base station using an orthogonal channel. On the other hand, the users inside the same sector are served using cooperative NOMA. This network architecture facilitates the cooperation of the paired NOMA users, as the near user is geographically located between the base station and the far user, when $M > 1$, and thus the near user is more likely to achieve a high cooperation gain, see [27], [28]. Without knowledge of the instantaneous channel gain at the base station, the paired NOMA users can be ordered based on their distances with respect to the base station. In fact, it has been shown in [11] that a higher performance gain can be achieved when users with more diverse channel conditions are paired. In light of this insight, we assume that the network coverage area is divided into two regions, i.e., an inner circle with radius $R_1 < R$ and an outer annulus, denoted by $\mathcal{A}_1$ and $\mathcal{A}_2$, respectively, as shown in Fig. 1.

As the users have the same spatial distribution in each sector, we focus on a typical sector, denoted as $\mathcal{C}(\beta)$, where $\beta = 2\pi/M$ is the angle of the sector. Note that $M = 1$ corresponds to the special case where the base station uses a single antenna to serve all users within the network coverage area. We pair one user in $\mathcal{A}_1 \cap \mathcal{C}(\beta)$ and one user in $\mathcal{A}_2 \cap \mathcal{C}(\beta)$ for NOMA transmission. Depending on the type of CSI (e.g., one-bit feedback or the users' distances) available at the base station, we consider two user pairing strategies, namely random user pairing in Section III and distance-based user pairing in Section IV.

B. Signal Model

The time is slotted into intervals of equal length. Within one time slot, the base station's codewords span K blocks of length T symbols each, where T depends on the length of the codewords. The DDF-based cooperative NOMA transmission involves two phases. In the first phase, the near user operates in the listening mode and receives the superimposed mixture of the users' signals transmitted by the base station. At a certain time instant, referred to as the *decision time*, the near user can successfully decode its own signal after having successfully decoded the signal intended for the far user. This is possible when the achievable rates of the near and the far users' signals at the near user exceed the target data rates of the near and the far users, respectively. In the second phase, from the decision time to the end of the time slot, the near user switches to the transmit mode and acts as a relay to help the far user decode its own signal. Thereby, the decision time is a random variable, which depends on the instantaneous channel gain between the near user and the base station. Without loss of generality, the decision time is assumed to coincide with the end of a block and is denoted as $\mathcal{D}$, which takes on values from the set $\{1, 2, \ldots, K\}$, as in [23]–[25]. Specifically, $1 \leq \mathcal{D} < K$ corresponds to the case that the near user assists the far user during the last $K - \mathcal{D}$ blocks, while $\mathcal{D} = K$ corresponds to the case where the near user is in the listening mode during the entire time slot.

We denote the paired NOMA users inside sector $\mathcal{C}(\beta)$ as $u_{\rm f}$ and $u_{\rm n}$, which denote the far user and the near user, respectively. When NOMA is performed to serve users $u_{\rm f}$ and $u_{\rm n}$, the i-th symbol transmitted by base station S can be expressed as

$$\hat{x}_{S,i} = \alpha_{\rm f}\sqrt{P_S}s_{{\rm f},i} + \alpha_{\rm n}\sqrt{P_S}s_{{\rm n},i}, \quad i = 1, 2, \ldots, KT, \tag{1}$$

where P_S denotes the transmit power of base station S, $\alpha_{\rm f}$ and $\alpha_{\rm n}$ denote the transmit power allocation coefficients for users $u_{\rm f}$ and $u_{\rm n}$, respectively, with $\alpha_{\rm f}^2 + \alpha_{\rm n}^2 = 1$, and $s_{{\rm f},i}$ and $s_{{\rm n},i}$ denote the i-th symbols transmitted to users $u_{\rm f}$ and $u_{\rm n}$, respectively, with $\mathbb{E}\left(|s_{\nu,i}|^2\right) = 1, \nu \in \{{\rm f}, {\rm n}\}$.

In the first phase of transmission, the signal received at user $u_\nu, \nu \in \{{\rm f}, {\rm n}\}$, is given by

$$y_{\nu,i} = \left(\alpha_{\rm f}\sqrt{P_S}s_{{\rm f},i} + \alpha_{\rm n}\sqrt{P_S}s_{{\rm n},i}\right) h_\nu \sqrt{\ell(x_\nu)} + z_{\nu,i}, \quad i = 1, 2, \ldots, \mathcal{D}T, \ \ \mathcal{D} \leq K, \tag{2}$$

where h_ν denotes the Rayleigh fading coefficient between base station S and user u_ν, and $\{z_{\nu,i}\}$ denotes the additive white Gaussian noise (AWGN) at user u_ν with zero mean and variance σ^2. Hence, $|h_\nu|^2$ is an exponential random variable with unit mean. In addition, $\ell(x_\nu) = r_\nu^{-\eta}$ and r_ν denote the path loss and the distance between base station S and user u_ν, respectively, where η is the path loss exponent, x_ν denotes the polar coordinate (r_ν, τ_ν) of the location of user u_ν, and τ_ν

denotes the angle of user u_ν with respect to base station S. The paired NOMA users are ordered based on their distances with respect to the base station. As $r_{\mathrm{n}} \leq r_{\mathrm{f}}$, we adopt $\alpha_{\mathrm{n}} \leq \alpha_{\mathrm{f}}$, i.e., the far user is assigned more power. Based on (2), the signal-to-interference-plus-noise ratio (SINR) of signal $\{s_{\mathrm{f},i}\}$ observed at the near user u_{n} is given by

$$\Gamma_{\mathrm{f}\to\mathrm{n}} = \frac{\alpha_{\mathrm{f}}^2 P_S |h_{\mathrm{n}}|^2 \ell(x_{\mathrm{n}})}{\alpha_{\mathrm{n}}^2 P_S |h_{\mathrm{n}}|^2 \ell(x_{\mathrm{n}}) + \sigma^2}, \tag{3}$$

where $\alpha_{\mathrm{f}}^2 P_S |h_{\mathrm{n}}|^2 \ell(x_{\mathrm{n}})$ and $\alpha_{\mathrm{n}}^2 P_S |h_{\mathrm{n}}|^2 \ell(x_{\mathrm{n}})$ denote the powers of the signals intended for the far user and the near user observed at the near user, respectively.

We denote the target data rates of the far and the near users as $R_{\mathrm{f}}^{\mathrm{th}}$ and $R_{\mathrm{n}}^{\mathrm{th}}$, respectively. If the achievable rate of the far user's signal at the near user exceeds the target data rate of the far user, i.e., $\frac{k}{K}\log_2\left(1+\Gamma_{\mathrm{f}\to\mathrm{n}}\right) \geq R_{\mathrm{f}}^{\mathrm{th}}, k=\{1,2,\ldots\}$, then the near user can successfully decode signal $\{s_{\mathrm{f},i}\}$. Subsequently, the near user can perform SIC to remove signal $\{s_{\mathrm{f},i}\}$ from the received signal $\{y_{\mathrm{n},i}\}$ and decode signal $\{s_{\mathrm{n},i}\}$ based on the signal-to-noise ratio (SNR) given by

$$\Gamma_{\mathrm{n}} = \frac{\alpha_{\mathrm{n}}^2 P_S \left|h_{\mathrm{n}}\right|^2 \ell(x_{\mathrm{n}})}{\sigma^2}. \tag{4}$$

The near user can successfully decode its own signal if $\frac{k'}{K}\log_2\left(1+\Gamma_{\mathrm{n}}\right) \geq R_{\mathrm{n}}^{\mathrm{th}}$, where $k' = \{k, k+1, \ldots\}$. If the near user cannot decode signal $\{s_{\mathrm{f},i}\}$ within K blocks, then the near user cannot perform SIC and cannot decode its own signal, i.e., an outage occurs.

On the other hand, by treating signal $\{s_{\mathrm{n},i}\}$ as co-channel interference, the SINR of signal $\{s_{\mathrm{f},i}\}$ observed at the far user u_{f} in the first phase of transmission can be expressed as

$$\Gamma_{\mathrm{f|n}}^{\mathrm{I}} = \frac{\alpha_{\mathrm{f}}^2 P_S |h_{\mathrm{f}}|^2 \ell(x_{\mathrm{f}})}{\alpha_{\mathrm{n}}^2 P_S |h_{\mathrm{f}}|^2 \ell(x_{\mathrm{f}}) + \sigma^2}. \tag{5}$$

According to the principle of DDF relaying, the near user switches from the listening mode to the transmit mode once it has successfully decoded both signals $\{s_{\mathrm{f},i}\}$ and $\{s_{\mathrm{n},i}\}$ received from base station S. Hence, the decision time can be written as

$$\mathcal{D} = \min\Bigg\{K, \min\Bigg\{k \,\Bigg|\, \frac{k}{K}\log_2\left(1+\Gamma_{\mathrm{f}\to\mathrm{n}}\right) \geq R_{\mathrm{f}}^{\mathrm{th}}, \\ \frac{k}{K}\log_2\left(1+\Gamma_{\mathrm{n}}\right) \geq R_{\mathrm{n}}^{\mathrm{th}}, k=\{1,2,\ldots\}\Bigg\}\Bigg\}. \tag{6}$$

After successfully decoding both signals $\{s_{\mathrm{f},i}\}$ and $\{s_{\mathrm{n},i}\}$ within $\mathcal{D}$ blocks, the near user can correctly predict the future transmit symbols of the base station (i.e., $s_{\mathrm{f},i}$ for $\mathcal{D}T+1 \leq i \leq KT$) since it knows the base station's codebook [24]. Based on this knowledge, the near user transmits the following signal in the second phase:

$$\tilde{s}_{\mathrm{f},i} = \begin{cases} s_{\mathrm{f},i+1}^*, & i = \mathcal{D}T+1, \mathcal{D}T+3, \ldots, KT-1, \\ -s_{\mathrm{f},i-1}^*, & i = \mathcal{D}T+2, \mathcal{D}T+4, \ldots, KT. \end{cases} \tag{7}$$

Base station S is unaware of the mode change at the near user and keeps transmitting the superimposed signal in the second phase. The base station and the near user transmit synchronously from the decision time to the end of the time slot. Hence, the signal received at the far user within blocks $[\mathcal{D}T+1, KT]$ reduces to an Alamouti constellation [29] and can be expressed as

$$y_{\mathrm{f},i} = \begin{cases} \left(\alpha_{\mathrm{f}}\sqrt{P_S}s_{\mathrm{f},i} + \alpha_{\mathrm{n}}\sqrt{P_S}s_{\mathrm{n},i}\right) h_{\mathrm{f}}\sqrt{\ell(x_{\mathrm{f}})} \\ \quad +\sqrt{P_U}s_{\mathrm{f},i+1}^* h_{\mathrm{f,n}}\sqrt{\ell(x_{\mathrm{f}}-x_{\mathrm{n}})} + z_{\mathrm{f},i}, \\ \quad i = \mathcal{D}T+1, \mathcal{D}T+3, \ldots, KT-1, \\ \left(\alpha_{\mathrm{f}}\sqrt{P_S}s_{\mathrm{f},i} + \alpha_{\mathrm{n}}\sqrt{P_S}s_{\mathrm{n},i}\right) h_{\mathrm{f}}\sqrt{\ell(x_{\mathrm{f}})} \\ \quad -\sqrt{P_U}s_{\mathrm{f},i-1}^* h_{\mathrm{f,n}}\sqrt{\ell(x_{\mathrm{f}}-x_{\mathrm{n}})} + z_{\mathrm{f},i}, \\ \quad i = \mathcal{D}T+2, \mathcal{D}T+4, \ldots, KT, \end{cases} \tag{8}$$

where P_U denotes the transmit power of the near user, and $h_{\mathrm{f,n}}$ and $\ell\left(x_{\mathrm{f}}-x_{\mathrm{n}}\right)$ denote the Rayleigh fading coefficient and the distance between users u_{f} and u_{n}, respectively. The far user exploits the signal received from both the base station and the near user for signal decoding. This resembles the decoding in hybrid automatic repeat request (HARQ) systems.

For simplicity of notation, we define $h_1 = \alpha_{\mathrm{f}}\sqrt{P_S}h_{\mathrm{f}}\sqrt{\ell(x_{\mathrm{f}})}$, $h_2 = \sqrt{P_{\mathrm{U}}}h_{\mathrm{f,n}}\sqrt{\ell(x_{\mathrm{f}}-x_{\mathrm{n}})}$, and $h_3 = \alpha_{\mathrm{n}}\sqrt{P_S}h_{\mathrm{f}}\sqrt{\ell(x_{\mathrm{f}})}$. Hence, for $i = \mathcal{D}T+1, \mathcal{D}T+3, \ldots, KT-1$, (8) can be rewritten as

$$y_{\mathrm{f},i} = h_1 s_{\mathrm{f},i} + h_3 s_{\mathrm{n},i} + h_2 s_{\mathrm{f},i+1}^* + z_{\mathrm{f},i}, \tag{9}$$

$$y_{\mathrm{f},i+1} = h_1 s_{\mathrm{f},i+1} + h_3 s_{\mathrm{n},i+1} - h_2 s_{\mathrm{f},i}^* + z_{\mathrm{f},i+1}. \tag{10}$$

For decoding, the received signal at the far user in (9) and (10) is linearly processed as [29]

$$\tilde{y}_{\mathrm{f},i} = y_{\mathrm{f},i}h_1^* - y_{\mathrm{f},i+1}^* h_2, \tag{11}$$

$$\tilde{y}_{\mathrm{f},i+1} = y_{\mathrm{f},i}^* h_2 + y_{\mathrm{f},i+1}h_1^*. \tag{12}$$

By substituting (9), (10) into (11), (12), we obtain

$$\tilde{y}_{\mathrm{f},i} = \left(\left|h_1\right|^2 + \left|h_2\right|^2\right) s_{\mathrm{f},i} + h_3 h_1^* s_{\mathrm{n},i} - h_3^* h_2 s_{\mathrm{n},i+1}^* + z_{\mathrm{f},i}h_1^* \\ -z_{\mathrm{f},i+1}^* h_2, \; i = \mathcal{D}T+1, \mathcal{D}T+3, \ldots, KT-1, \tag{13}$$

$$\tilde{y}_{\mathrm{f},i} = \left(\left|h_1\right|^2 + \left|h_2\right|^2\right) s_{\mathrm{f},i} + h_3^* h_2 s_{\mathrm{n},i-1}^* + h_3 h_1^* s_{\mathrm{n},i} \\ +z_{\mathrm{f},i-1}^* h_2 + z_{\mathrm{f},i}h_1^*, i = \mathcal{D}T+2, \mathcal{D}T+4, \ldots, KT. \tag{14}$$

By substituting h_1, h_2, and h_3 into (13), (14), we have

$$\tilde{y}_{\mathrm{f},i} = \left(\alpha_{\mathrm{f}}^2 P_S |h_{\mathrm{f}}|^2 \ell(x_{\mathrm{f}}) + P_U |h_{\mathrm{f,n}}|^2 \ell(x_{\mathrm{f}}-x_{\mathrm{n}})\right) s_{\mathrm{f},i} + \tilde{z}_{\mathrm{f},i}, \\ i = \mathcal{D}T+1, \ldots, KT, \tag{15}$$

where $\tilde{z}_{\mathrm{f},i}$ is given in (16), shown at the top of the next page.

From (15) and (16), the SINR of signal $\{s_{\mathrm{f},i}\}$ observed at the far user u_{f} in the second phase of transmission can be expressed as

$$\Gamma_{\mathrm{f|n}}^{\mathrm{II}} = \frac{\alpha_{\mathrm{f}}^2 P_S |h_{\mathrm{f}}|^2 \ell(x_{\mathrm{f}}) + P_U |h_{\mathrm{f,n}}|^2 \ell(x_{\mathrm{f}}-x_{\mathrm{n}})}{\alpha_{\mathrm{n}}^2 P_S |h_{\mathrm{f}}|^2 \ell(x_{\mathrm{f}}) + \sigma^2}. \tag{17}$$

Based on the above signal reception model, the SINR of signal $\{s_{\mathrm{f},i}\}$ observed at the far user u_{f} depends on whether the near user is in the listening or in the transmit mode. Hence, the achievable rate at the far user u_{f} during the entire time slot can be expressed as

$$R_{\mathrm{f}} = \begin{cases} \frac{\mathcal{D}}{K}\log_2\left(1+\Gamma_{\mathrm{f|n}}^{\mathrm{I}}\right) + \frac{K-\mathcal{D}}{K}\log_2\left(1+\Gamma_{\mathrm{f|n}}^{\mathrm{II}}\right), \\ \qquad\qquad \text{if } 1 \leq \mathcal{D} < K, \\ \log_2\left(1+\Gamma_{\mathrm{f|n}}^{\mathrm{I}}\right), \qquad \text{if } \mathcal{D} = K, \end{cases} \tag{18}$$

$$\tilde{z}_{\mathrm{f},i}=\begin{cases}\alpha_{\mathrm{f}}\alpha_{\mathrm{n}}P_S\ell(x_{\mathrm{f}})\left|h_{\mathrm{f}}\right|^2 s_{\mathrm{n},i}-\alpha_{\mathrm{n}}\sqrt{P_SP_U\ell(x_{\mathrm{f}})\ell(x_{\mathrm{f}}-x_{\mathrm{n}})}h_{\mathrm{f}}^*h_{\mathrm{f,n}}s_{\mathrm{n},i+1}^*\\ \quad+\alpha_{\mathrm{f}}\sqrt{P_S\ell(x_{\mathrm{f}})}h_{\mathrm{f}}^*z_{\mathrm{f},i}-\sqrt{P_U\ell(x_{\mathrm{f}}-x_{\mathrm{n}})}h_{\mathrm{f,n}}z_{\mathrm{f},i+1}^*, i=\mathcal{D}T+1,\mathcal{D}T+3,\ldots,KT-1,\\ \alpha_{\mathrm{n}}\sqrt{P_SP_U\ell(x_{\mathrm{f}})\ell(x_{\mathrm{f}}-x_{\mathrm{n}})}h_{\mathrm{f}}^*h_{\mathrm{f,n}}s_{\mathrm{n},i-1}^*+\alpha_{\mathrm{f}}\alpha_{\mathrm{n}}P_S\ell(x_{\mathrm{f}})|h_{\mathrm{f}}|^2s_{\mathrm{n},i}\\ \quad+\sqrt{P_U\ell(x_{\mathrm{f}}-x_{\mathrm{n}})}h_{\mathrm{f,n}}z_{\mathrm{f},i-1}^*+\alpha_{\mathrm{f}}\sqrt{P_S\ell(x_{\mathrm{f}})}h_{\mathrm{f}}^*z_{\mathrm{f},i}, i=\mathcal{D}T+2,\mathcal{D}T+4,\ldots,KT.\end{cases}\tag{16}$$

---

where $\Gamma_{\mathrm{f|n}}^{\mathrm{I}}$ and $\Gamma_{\mathrm{f|n}}^{\mathrm{II}}$ are given in (5) and (17), respectively.

In the following two sections, we derive the probability mass function of the decision time, the outage probability, the diversity order, and the sum rate of the proposed DDF-based cooperative NOMA scheme for random and distance-based user pairing strategies, respectively.

III. Random User Pairing

In this section, we consider DDF-based cooperative NOMA with random user pairing, where base station S randomly pairs one user in $\mathcal{A}_1\cap\mathcal{C}(\beta)$ and one user in $\mathcal{A}_2\cap\mathcal{C}(\beta)$ for downlink cooperative NOMA transmission based on one-bit feedback. Specifically, each user feeds back 1 or 0 to base station S to indicate whether it is located in $\mathcal{A}_1\cap\mathcal{C}(\beta)$ or $\mathcal{A}_2\cap\mathcal{C}(\beta)$. Under the random user pairing strategy, each user has the same opportunity to be served. Note that when there is either no near or no far user, OMA can be employed by the base station to serve the randomly selected far or near user. As the performance analysis of DDF-based cooperative NOMA is the main focus of this paper and the performance analysis of OMA is straightforward, we assume that there exist at least one near user and one far user.

A. Probability Mass Function of Decision Time

For notational ease, we define $\theta(R_{\mathrm{f}}^{\mathrm{th}},k)=2^{\frac{R_{\mathrm{f}}^{\mathrm{th}}K}{k}}-1$, which can be interpreted as the SINR reception threshold given the target data rate $R_{\mathrm{f}}^{\mathrm{th}}$ and the number of blocks k. If $\alpha_{\mathrm{f}}^2>\theta(R_{\mathrm{f}}^{\mathrm{th}},k)\alpha_{\mathrm{n}}^2$, the probability that the near user u_{n} can successfully decode both signals $\{s_{\mathrm{f},i}\}$ and $\{s_{\mathrm{n},i}\}$ received from base station S after being in the listening mode for the first $k\in\{1,\ldots,K\}$ blocks can be written as

$$\begin{aligned}&D_T(k)\\&=\mathbb{P}\left(\frac{k}{K}\log_2\left(1+\Gamma_{\mathrm{f\to n}}\right)\ge R_{\mathrm{f}}^{\mathrm{th}},\frac{k}{K}\log_2\left(1+\Gamma_{\mathrm{n}}\right)\ge R_{\mathrm{n}}^{\mathrm{th}}\right)\\&\overset{(a)}{=}\mathbb{P}\left(|h_{\mathrm{n}}|^2\ge\max\left\{\frac{\theta(R_{\mathrm{f}}^{\mathrm{th}},k)\sigma^2}{\left(\alpha_{\mathrm{f}}^2-\theta(R_{\mathrm{f}}^{\mathrm{th}},k)\alpha_{\mathrm{n}}^2\right)P_S\ell(x_{\mathrm{n}})},\right.\right.\\&\qquad\left.\left.\frac{\theta(R_{\mathrm{n}}^{\mathrm{th}},k)\sigma^2}{\alpha_{\mathrm{n}}^2P_S\ell(x_{\mathrm{n}})}\right\}\right)\\&\overset{(b)}{=}\mathbb{E}_{x_{\mathrm{n}}}\left(\exp\left(-G(k)r_{\mathrm{n}}^{\eta}\right)\right),\end{aligned}\tag{19}$$

where (a) follows by substituting (3) and (4), (b) follows by taking the expectation over the exponential distribution of channel gain $|h_{\mathrm{n}}|^2$, and we define

$$G(k)=\frac{\sigma^2}{P_S}\max\left\{\frac{\theta(R_{\mathrm{f}}^{\mathrm{th}},k)}{\alpha_{\mathrm{f}}^2-\theta(R_{\mathrm{f}}^{\mathrm{th}},k)\alpha_{\mathrm{n}}^2},\frac{\theta(R_{\mathrm{n}}^{\mathrm{th}},k)}{\alpha_{\mathrm{n}}^2}\right\}.\tag{20}$$

On the other hand, if $\alpha_{\mathrm{f}}^2\le\theta(R_{\mathrm{f}}^{\mathrm{th}},k)\alpha_{\mathrm{n}}^2$, we have $G(k)=\infty$ and $D_T(k)=0$.

Due to random user pairing, the PDFs of distance r_{n} and angle τ_{n} of user u_{n} with respect to base station S are given by $f_{r_{\mathrm{n}}}(r)=2r/R_1^2$ and $f_{\tau_{\mathrm{n}}}(\tau)=1/\beta$, respectively. As a result, if $\alpha_{\mathrm{f}}^2>\theta(R_{\mathrm{f}}^{\mathrm{th}},k)\alpha_{\mathrm{n}}^2$, we have

$$\begin{aligned}D_T(k)&=\int_0^{\beta}\int_0^{R_1}\exp\left(-G(k)r_{\mathrm{n}}^{\eta}\right)\frac{2r_{\mathrm{n}}}{R_1^2}\mathrm{d}r_{\mathrm{n}}\frac{1}{\beta}\mathrm{d}\tau_{\mathrm{n}}\\&=\frac{2}{R_1^2\eta}\left(G(k)\right)^{-\frac{2}{\eta}}\gamma\left(\frac{2}{\eta},G(k)R_1^{\eta}\right),\end{aligned}\tag{21}$$

where $\gamma(a,b)=\int_0^b\exp(-c)c^{a-1}\mathrm{d}c$ is the lower incomplete Gamma function [30].

According to (6), the decision time is the minimum number of blocks required by the near user to successfully decode both signals $\{s_{\mathrm{f},i}\}$ and $\{s_{\mathrm{n},i}\}$ received from the base station. In other words, decision time $\mathcal{D}=k$ is equivalent to the event that the near user fails to successfully decode both signals after being in the listening mode for the first $(k-1)$ blocks but successfully decodes both signals after being in the listening mode for the first k blocks. Hence, the probability mass function of decision time $\mathcal{D}$, where $\mathcal{D}\in\{1,\ldots,K-1\}$, is given by

$$\begin{aligned}\mathbb{P}\left(\mathcal{D}=k\right)&=\mathbb{P}\left(\mathcal{D}\le k\right)-\mathbb{P}\left(\mathcal{D}\le k-1\right)\\&=D_T(k)-D_T(k-1)\\&\overset{(a)}{=}\frac{2}{R_1^2\eta}\left(\left(G(k)\right)^{-\frac{2}{\eta}}\gamma\left(\frac{2}{\eta},G(k)R_1^{\eta}\right)\right.\\&\qquad\left.-\left(G(k-1)\right)^{-\frac{2}{\eta}}\gamma\left(\frac{2}{\eta},G(k-1)R_1^{\eta}\right)\right),\end{aligned}\tag{22}$$

where (a) follows by substituting (21). As the near user cannot successfully decode any signal before the base station starts transmitting, we have $D_T(0)=0$. On the other hand, the probability that the decision time is $\mathcal{D}=K$ is given by

$$\begin{aligned}&\mathbb{P}\left(\mathcal{D}=K\right)\\&=1-D_T(K-1)\\&=1-\frac{2}{R_1^2\eta}\left(G(K-1)\right)^{-\frac{2}{\eta}}\gamma\left(\frac{2}{\eta},G(K-1)R_1^{\eta}\right).\end{aligned}\tag{23}$$

B. Outage Probability of Near User

An outage event occurs at the near user u_{n} when it fails to decode signal $\{s_{\mathrm{n},i}\}$ received from base station S after being in the listening mode for all K blocks. As the successful decoding of signal $\{s_{\mathrm{f},i}\}$ is a prerequisite for performing SIC and decoding signal $\{s_{\mathrm{n},i}\}$ at near user u_{n}, the outage probability of the near user can be expressed as

$$q_{\mathrm{out,n}}=\mathbb{P}\left(\log_2\left(1+\Gamma_{\mathrm{f\to n}}\right)<R_{\mathrm{f}}^{\mathrm{th}}\right)$$

$$+\mathbb{P}\left(\log_2\left(1+\Gamma_{\mathrm{f}\to\mathrm{n}}\right)\geq R_{\mathrm{f}}^{\mathrm{th}},\log_2\left(1+\Gamma_{\mathrm{n}}\right)<R_{\mathrm{n}}^{\mathrm{th}}\right),\quad(24)$$

where the first term is the probability that the near user u_{n} fails to decode signal $\{s_{\mathrm{f},i}\}$, and the second term represents the probability that the near user successfully decodes signal $\{s_{\mathrm{f},i}\}$ but fails to decode signal $\{s_{\mathrm{n},i}\}$ after applying SIC.

The outage probability is the complement of the probability of successful signal reception, which is the probability that the near user u_{n} can successfully decode both signals $\{s_{\mathrm{f},i}\}$ and $\{s_{\mathrm{n},i}\}$ within the entire time slot. Hence, the outage probability of the near user of the DDF-based cooperative NOMA scheme with random user pairing can be equivalently expressed as

$$\begin{aligned}q_{\mathrm{out,n}}&=1-D_T(K)\\&\overset{(a)}{=}1-\frac{2}{R_1^2\eta}\left(G(K)\right)^{-2/\eta}\gamma\left(\frac{2}{\eta},G(K)R_1^{\eta}\right),\quad(25)\end{aligned}$$

where (a) follows by substituting (21) with $k=K$.

C. Outage Probability of Far User

An outage event occurs at the far user u_{f} when it fails to decode signal $\{s_{\mathrm{f},i}\}$ within the entire time slot. This outage event can be divided into the following two cases: 1) Case I - The near user u_{n} fails to decode signals $\{s_{\mathrm{f},i}\}$ and $\{s_{\mathrm{n},i}\}$ after being in the listening mode for the first $K-1$ blocks, and the far user u_{f} also fails to decode signal $\{s_{\mathrm{f},i}\}$ received from the base station; 2) Case II - The near user u_{n} successfully decodes both signals $\{s_{\mathrm{f},i}\}$ and $\{s_{\mathrm{n},i}\}$ after being in the listening mode for the first $\mathcal{D}<K$ blocks, but the far user u_{f} fails to decode signal $\{s_{\mathrm{f},i}\}$ received from both the base station and the near user. The probabilities of Case I and Case II are denoted as $q_{\mathrm{out,f}}^{\mathrm{I}}$ and $q_{\mathrm{out,f}}^{\mathrm{II}}$, respectively. As a result, the outage probability of the far user of DDF-based cooperative NOMA with random user pairing can be expressed as

$$\begin{aligned}q_{\mathrm{out,f}}&=q_{\mathrm{out,f}}^{\mathrm{I}}+q_{\mathrm{out,f}}^{\mathrm{II}}\\&=\mathbb{P}\left(\mathcal{D}=K,\log_2\left(1+\Gamma_{\mathrm{f|n}}^{\mathrm{I}}\right)<R_{\mathrm{f}}^{\mathrm{th}}\right)\\&\quad+\mathbb{E}_{x_{\mathrm{n}},x_{\mathrm{f}}}\left(\sum_{k=1}^{K-1}Q_n\left(r_{\mathrm{n}},k\right)Q(k)\right),\quad(26)\end{aligned}$$

where

$$Q_n\left(r_{\mathrm{n}},k\right)=\exp\left(-G(k)r_{\mathrm{n}}^{\eta}\right)-\exp\left(-G(k-1)r_{\mathrm{n}}^{\eta}\right),\quad(27)$$

$$\begin{aligned}Q(k)=\mathbb{P}\Bigg(&\frac{k}{K}\log_2\left(1+\Gamma_{\mathrm{f|n}}^{\mathrm{I}}\right)\\&+\frac{K-k}{K}\log_2\left(1+\Gamma_{\mathrm{f|n}}^{\mathrm{II}}\right)<R_{\mathrm{f}}^{\mathrm{th}}\Bigg).\quad(28)\end{aligned}$$

Here, $Q_n(r_{\mathrm{n}},k)$ represents the probability that decision time $\mathcal{D}$ is equal to k when the distance between the near user u_{n} and base station S is r_{n}. The following proposition presents the approximate outage probability of the far user of the proposed DDF-based cooperative NOMA scheme with random user pairing.

Proposition 1. *Assuming the existence of at least one near user and one far user, the outage probability of the far user of the DDF-based cooperative NOMA scheme with random user pairing can be approximated as in (29), shown at the top of the next page, if $\alpha_{\mathrm{f}}^2>\theta\left(R_{\mathrm{f}}^{\mathrm{th}},K\right)\alpha_n^2$, otherwise $q_{\mathrm{out,f}}=1$, where $D_T(K-1)$ and $Q_n(r_{\mathrm{n},c},k)$ are given in (21) and (27), respectively, $C_1=\frac{\theta(R_{\mathrm{f}}^{\mathrm{th}},K)\sigma^2}{\left(\alpha_{\mathrm{f}}^2-\theta(R_{\mathrm{f}}^{\mathrm{th}},K)\alpha_{\mathrm{n}}^2\right)P_S}$, $\omega_c=\cos\left(\frac{2c-1}{2C}\pi\right)$, $r_{\mathrm{n},c}=\frac{R_1}{2}(\omega_c+1)$, $\zeta_l=\cos\left(\frac{2l-1}{2L}\pi\right)$, $\tau_{D,l}=\frac{\beta}{2}(\zeta_l+1)$, $\psi_j=\cos\left(\frac{2j-1}{2J}\pi\right)$, $r_{\mathrm{f},j}=\frac{R-R_1}{2}\psi_j+\frac{R+R_1}{2}$, $\phi_i=\cos\left(\frac{2i-1}{2I}\pi\right)$, $z_i=\frac{kR_{\mathrm{f}}^{\mathrm{th}}}{2K}(\phi_i+1)$, $Q_z(r_{\mathrm{f}},r_{\mathrm{n}},\tau_D,k)$ is given in (30), shown at the top of the next page,*

$$G_1(z,k)=\frac{\sigma^2\theta(z,k)}{\left(\alpha_{\mathrm{f}}^2-\theta(z,k)\alpha_{\mathrm{n}}^2\right)P_S},\quad(31)$$

$$G_2(z,k)=\frac{\alpha_{\mathrm{f}}^2\sigma^2\left(\theta(z,k)+1\right)K\ln 2}{\left(\alpha_{\mathrm{f}}^2-\theta(z,k)\alpha_{\mathrm{n}}^2\right)^2P_Sk},\quad(32)$$

$$G_3(z,k)=\frac{\sigma^2\alpha_{\mathrm{f}}^2\left(\theta\left(R_{\mathrm{f}}^{\mathrm{th}}-z,K-k\right)-\theta\left(z,k\right)\right)}{\left(\alpha_{\mathrm{f}}^2-\theta(z,k)\alpha_{\mathrm{n}}^2\right)P_U},\quad(33)$$

and C, I, J, and L are parameters to balance the tradeoff between the computational complexity and the accuracy of the approximation.

Proof. Please refer to Appendix A. □

The accuracy of the approximations in Proposition 1 is verified in Section V by computer simulations. According to Proposition 1, the outage probability of the far user of DDF-based cooperative NOMA with random user pairing depends on the target data rates of both the near and the far users ($R_{\mathrm{n}}^{\mathrm{th}}$ and $R_{\mathrm{f}}^{\mathrm{th}}$), as both target data rates determine the decision time of the near user and hence affect the achievable rate of the far user. Furthermore, the outage probability of the far user also depends on the spatial distribution of the users, the transmit power allocation coefficients (α_{f}^2 and α_{n}^2), the number of blocks in one time slot (K), and the path loss exponent (η). In particular, the transmit power allocation coefficients (α_{f}^2 and α_{n}^2) should be carefully set based on the choice of the target data rate of the far user ($R_{\mathrm{f}}^{\mathrm{th}}$), so as to ensure that the condition $\alpha_{\mathrm{f}}^2>\theta\left(R_{\mathrm{f}}^{\mathrm{th}},K\right)\alpha_n^2$ is satisfied and hence SIC can be successfully performed at the near user. The following corollary presents the outage probability of the far user of the DDF-based cooperative NOMA scheme with random user pairing in the high SNR regime.

Corollary 1. *For path loss exponent $\eta=2$, sector angle $\beta\leq\frac{\pi}{3}$, and high transmit SNRs $\frac{P_S}{\sigma^2}$ and $\frac{P_U}{\sigma^2}$, assuming the existence of at least one near user and one far user, the outage probability of the far user of the DDF-based cooperative NOMA scheme with random user pairing can be simplified as in (34), shown at the top of the next page, if $\alpha_{\mathrm{f}}^2>\theta\left(R_{\mathrm{f}}^{\mathrm{th}},K\right)\alpha_{\mathrm{n}}^2$, otherwise $q_{\mathrm{out,f}}=1$, where $k_{\min}=\lceil R_{\mathrm{f}}^{\mathrm{th}}K/\log_2\left(1+\alpha_{\mathrm{f}}^2/\alpha_{\mathrm{n}}^2\right)\rceil$, $k_{\max}=\lceil 0.9K\rceil$, $A_1(z_i,k)=\frac{R^4-R_1^4}{4}-G_1(z_i,k)\frac{R^6-R_1^6}{6}$, $A_2(z_i,k)=\left(2-\frac{\beta^2}{6}\right)\left(G_1(z_i,k)\frac{R^7-R_1^7}{7}-\frac{R^5-R_1^5}{5}\right)$, $A_3(z_i,k)=\frac{R^6-R_1^6}{6}-G_1(z_i,k)\frac{R^8-R_1^8}{8}$, $A_4(z_i,k)=\frac{A_1(z_i,k)R_1^2}{6}+\frac{A_2(z_i,k)R_1}{5}+\frac{A_3(z_i,k)}{4}$, $A_5(z_i,k)=\frac{A_1(z_i,k)}{4}+\frac{A_2(z_i,k)}{3R_1}+\frac{A_3(z_i,k)}{2R_1^2}$, $\phi_i=\cos\left(\frac{2i-1}{2I}\pi\right)$, $z_i=\frac{kR_{\mathrm{f}}^{\mathrm{th}}}{2K}(\phi_i+1)$, and*

$$q_{\mathrm{out,f}}^{\mathrm{I}}=\left(1-D_T(K-1)\right)\left(1-\frac{2}{\eta\left(R^2-R_1^2\right)}C_1^{-2/\eta}\right.$$

$$q_{\text{out,f}} \approx (1 - D_T(K-1)) \left(1 - \frac{2}{\eta\left(R^2 - R_1^2\right)} C_1^{-2/\eta} \left(\gamma\left(\frac{2}{\eta}, C_1 R^\eta\right) - \gamma\left(\frac{2}{\eta}, C_1 R_1^\eta\right)\right)\right)$$
$$+ \frac{\pi^3}{(R+R_1)R_1\beta CLJ} \sum_{c=1}^{C} \sqrt{1-\omega_c^2} \sum_{k=1}^{K-1} Q_n(r_{\text{n},c}, k) \sum_{l=1}^{L} \sqrt{1-\zeta_l^2} \sum_{j=1}^{J} \sqrt{1-\psi_j^2} Q_z(r_{\text{f},j}, r_{\text{n},c}, \tau_{D,l}, k) r_{\text{f},j}^{\eta+1} (\beta - \tau_{D,l}) r_{\text{n},c}, \quad (29)$$

$$Q_z(r_\text{f}, r_\text{n}, \tau_D, k) \approx \frac{k R_\text{f}^{\text{th}} \pi}{2KI} \sum_{i=1}^{I} \left(\sqrt{1-\phi_i^2} \left(1 - \exp\left(-G_3(z_i,k)\left(r_\text{f}^2 + r_\text{n}^2 - 2 r_\text{f} r_\text{n} \cos\tau_D\right)^{\eta/2}\right)\right) \times \exp\left(-G_1(z_i,k) r_\text{f}^\eta\right) G_2(z_i,k) \right), \quad (30)$$

$$q_{\text{out,f}} \approx q_{\text{out,f}}^{\text{I}} + \frac{2R_1^2 R_\text{f}^{\text{th}} \pi}{\left(R^2 - R_1^2\right) KI} \left(\sum_{k=k_{\min}+1}^{k_{\max}} k\left(G(k-1) - G(k)\right) \sum_{i=1}^{I} \sqrt{1-\phi_i^2} G_2(z_i,k) G_3(z_i,k) A_4(z_i,k) + \sum_{i=1}^{I} \sqrt{1-\phi_i^2} G_2(z_i,k_{\min}) G_3(z_i,k_{\min}) \left(A_5(z_i,k_{\min}) - G(k_{\min}) A_4(z_i,k_{\min})\right) \right), \quad (34)$$

$$\times \left(\gamma\left(\frac{2}{\eta}, C_1 R^\eta\right) - \gamma\left(\frac{2}{\eta}, C_1 R_1^\eta\right)\right)\Bigg). \quad (35)$$

Proof. Please refer to Appendix B. □

In (34), functions $A_4(z_i,k)$ and $A_5(z_i,k)$ depend on β only via $A_2(z_i,k)$, and all other terms do not depend on β. Hence, after some algebraic manipulations, we can express the outage probability of the far user in the high SNR regime as a function of β^2 as follows

$$q_{\text{out,f}} \approx B_1 \beta^2 + B_2, \quad (36)$$

where $B_1 > 0$ and $B_2 > 0$ are constants which do not depend on β. In general, outage probability $q_{\text{out,f}}$ depends on sector angle β because the distance between the paired near and far users depends on β. Eq. (36) reveals that a smaller value of β leads to a lower outage probability.

The high SNR approximations (i.e., (69) and (70)) derived in the proof of Corollary 1 can be used to derive the diversity order for the far user. We denote the transmit SNRs $\frac{P_S}{\sigma^2} = \frac{P_U}{\sigma^2} = \rho$. Based on (54), when $\rho \to \infty$, we have

$$q_{\text{out,f}}^{\text{I}} \overset{(a)}{\approx} \mathbb{E}_{x_n}\left(G(K-1) r_\text{n}^\eta\right) \mathbb{E}_{x_\text{f}}\left(C_1 r_\text{f}^\eta\right) \overset{(b)}{\sim} \frac{1}{\rho^2}, \quad (37)$$

where (a) follows by applying $\exp(-x) \approx 1 - x$ when $x \to 0$, and (b) follows as both $G(K-1)$ and C_1 are directly proportional to $1/\rho$, i.e., $G(K-1) \sim 1/\rho$ and $C_1 \sim 1/\rho$. Hence, $q_{\text{out,f}}^{\text{I}}$ decreases at a rate of $1/\rho^2$.

On the other hand, by substituting (69) and (70) into (64), we obtain that $q_{\text{out,f}}^{\text{II}}$ decreases at a rate of $1/\rho^3$, i.e., $q_{\text{out,f}}^{\text{II}} \sim 1/\rho^3$, as $G(k)$, $G_2(z,k)$, and $G_3(z,k)$ are directly proportional to $1/\rho$. As $q_{\text{out,f}} = q_{\text{out,f}}^{\text{I}} + q_{\text{out,f}}^{\text{II}}$, we have $q_{\text{out,f}} \sim 1/\rho^2$. Hence, the diversity order achieved by the far user u_f of DDF-based cooperative NOMA with random user pairing can be calculated as

$$D_\text{f}^{\text{O}} = \lim_{\rho\to\infty} \frac{-\log_2(q_{\text{out,f}})}{\log_2 \rho} = 2. \quad (38)$$

In comparison, the diversity orders achieved by the far user of both conventional NOMA with random user pairing [12] and OMA are one, as the far user only receives one copy of its signal from the base station. The diversity order of the far user of cooperative NOMA [17] is two at the cost of reducing spectral efficiency, as discussed in Section V. By adapting to the instantaneous channel conditions, the proposed DDF-based cooperative NOMA scheme can achieve a diversity order of two for the far user without sacrificing spectral efficiency while realizing superposition transmission, and hence obtain a better outage performance. Employing a similar analysis as for the far user, we can show that the diversity order for the near user of DDF-based cooperative NOMA with random user pairing is one.

The following corollary provides a simplified expression for the outage probability of the far user when $R_1 \ll R$, which can be more efficiently calculated than the expression in (29).

Corollary 2. *For the special case of $R_1 \ll R$, assuming the existence of at least one near user and one far user, the outage probability of the far user of the DDF-based cooperative NOMA scheme with random user pairing can be simplified as*

$$q_{\text{out,f}} \approx q_{\text{out,f}}^{\text{I}} + \frac{2R_\text{f}^{\text{th}}\pi}{\left(R^2 - R_1^2\right) R_1^2 KI} \sum_{k=1}^{K-1} k\Delta_1(k) \times \left(\sum_{i=1}^{I} \sqrt{1-\phi_i^2} \Delta_2(z_i,k) G_2(z_i,k) \right), \quad (39)$$

$$\Delta_2(z_i,k)=\frac{1}{\eta}(G_1(z_i,k))^{-\frac{\eta+2}{\eta}}\left(\gamma\left(\frac{\eta+2}{\eta},G_1(z_i,k)R^\eta\right)-\gamma\left(\frac{\eta+2}{\eta},G_1(z_i,k)R_1^\eta\right)\right)$$
$$-\frac{1}{\eta}\left(G_1(z_i,k)+G_3(z_i,k)\right)^{-\frac{\eta+2}{\eta}}\gamma\left(\frac{\eta+2}{\eta},\left(G_1(z_i,k)+G_3(z_i,k)\right)R^\eta\right)$$
$$-\frac{1}{\eta}\left(G_1(z_i,k)+G_3(z_i,k)\right)^{-\frac{\eta+2}{\eta}}\gamma\left(\frac{\eta+2}{\eta},\left(G_1(z_i,k)+G_3(z_i,k)\right)R_1^\eta\right). \quad (40)$$

if $\alpha_{\rm f}^2>\theta\left(R_{\rm f}^{\rm th},K\right)\alpha_{\rm n}^2$, *otherwise* $q_{\rm out,f}=1$, *where* $q_{\rm out,f}^{\rm I}$ *is given in (35),* $\phi_i=\cos\left(\frac{2i-1}{2I}\pi\right)$, $z_i=\frac{kR_{\rm f}^{\rm th}}{2K}(\phi_i+1)$, $\Delta_1(k)=\frac{1}{\eta}\left(G(k)\right)^{-2/\eta}\gamma\left(\frac{2}{\eta},G(k)R_1^\eta\right)-\frac{1}{\eta}\left(G(k-1)\right)^{-2/\eta}\gamma\left(\frac{2}{\eta},G(k-1)R_1^\eta\right)$, *and* $\Delta_2(z_i,k)$ *is given in (40), shown at the top of this page.*

Proof. If $R_1\ll R$, we have $\left(r_{\rm f}^2+r_{\rm n}^2-2r_{\rm f}r_{\rm n}\cos\tau_D\right)^{\eta/2}\approx r_{\rm f}^\eta$. In this case, the integrals over τ_D, $r_{\rm f}$, and $r_{\rm n}$ in (64) can be separated. By separately calculating each integral and applying the Gauss-Chebyshev quadrature, we obtain (39). The details of the calculation of the integrals are omitted due to space limitation. □

Corollary 2 reveals that although the outage probability of the far user in general depends on sector angle β, cf. (36), for the special case of $R_1\ll R$, it becomes independent of β. This is due to the fact that for $R_1\ll R$, the distance between the far user and the near user becomes independent of β.

D. Sum Rate

The base station transmits the signals to the near and the far users with target data rates $R_{\rm n}^{\rm th}$ and $R_{\rm f}^{\rm th}$, respectively. Hence, the sum rate is determined by the outage probability. Assuming the existence of at least one near user and one far user in sector $\mathcal{C}(\beta)$, the sum rate of the DDF-based cooperative NOMA scheme with random user pairing is given by

$$R_{\rm sum}=\left(1-q_{\rm out,n}\right)R_{\rm n}^{\rm th}+\left(1-q_{\rm out,f}\right)R_{\rm f}^{\rm th}, \quad (41)$$

where $q_{\rm out,n}$ and $q_{\rm out,f}$ are given in (25) and (29), respectively.

IV. Distance-Based User Pairing

In this section, we consider DDF-based cooperative NOMA with distance-based user pairing, where the base station is assumed to know the users' distance information. Compared to the instantaneous channel gain, a user's distance changes relatively slower and hence is more practical for the base station to obtain. We focus on the typical sector $\mathcal{C}(\beta)$. The number of users inside $\mathcal{A}_1\cap\mathcal{C}(\beta)$ and $\mathcal{A}_2\cap\mathcal{C}(\beta)$ are denoted as $N_{\rm n}$ and $N_{\rm f}$, respectively. With the users' distances, base station S orders the users based on the following criterion:

$$r_{{\rm n},1}\le r_{{\rm n},2}\le\cdots\le r_{{\rm n},m}\le\cdots\le r_{{\rm n},N_{\rm n}}, \quad (42)$$
$$r_{{\rm f},1}\le r_{{\rm f},2}\le\cdots\le r_{{\rm f},v}\le\cdots\le r_{{\rm f},N_{\rm f}}, \quad (43)$$

where $r_{{\rm n},m}$ denotes the distance between base station S and the m-th nearest user in $\mathcal{A}_1\cap\mathcal{C}(\beta)$, and $r_{{\rm f},v}$ denotes the distance between base station S and the v-th nearest user in $\mathcal{A}_2\cap\mathcal{C}(\beta)$.

To investigate the impact of the paired NOMA users' locations on the network performance, we consider a general user pair, where base station S pairs the m-th nearest user inside $\mathcal{A}_1\cap\mathcal{C}(\beta)$, denoted as $u_{{\rm n},m}$, and the v-th nearest user inside $\mathcal{A}_2\cap\mathcal{C}(\beta)$, denoted as $u_{{\rm f},v}$, for downlink cooperative NOMA transmission. In the following, we derive the probability mass function of the decision time, the outage probabilities of the near and the far users, the diversity order, and the sum rate of the DDF-based cooperative NOMA scheme for distance-based user pairing.

A. Probability Mass Function of Decision Time

Assuming that there are at least m users inside $\mathcal{A}_1\cap\mathcal{C}(\beta)$, the complementary CDF (CCDF) of distance $r_{{\rm n},m}$ is equal to the probability that there are less than m users inside a sector with radius r, where $r\le R_1$, denoted by $\mathcal{C}(r,\beta)$. Hence, we have

$$\overline{F}_{r_{{\rm n},m}}(r)\overset{(a)}{=}\mathbb{P}\left(\sum_{x_i\in\Phi}\mathbb{1}\left(x_i\in\mathcal{C}(r,\beta)\right)<m\,\middle|\,N_{\rm n}\ge m\right)$$
$$\overset{(b)}{=}\frac{\mathbb{P}\left(\sum_{x_i\in\Phi}\mathbb{1}\left(x_i\in\mathcal{C}(r,\beta)\right)<m,N_{\rm n}\ge m\right)}{\mathbb{P}\left(N_{\rm n}\ge m\right)}$$
$$\overset{(c)}{=}\frac{1}{\mathbb{P}\left(N_{\rm n}\ge m\right)}\sum_{j=1}^{m-1}\frac{1}{j!}\left(\frac{\lambda\beta r^2}{2}\right)^j\exp\left(-\frac{\lambda\beta r^2}{2}\right)$$
$$\times\left(1-\sum_{b=0}^{m-j-1}\frac{1}{b!}\left(\frac{\lambda\beta(R_1^2-r^2)}{2}\right)^b\exp\left(-\frac{\lambda\beta(R_1^2-r^2)}{2}\right)\right), \quad (44)$$

where $\mathbb{1}(\cdot)$ is the indicator function, (a) follows from the definition of intensity measure [26], (b) follows from the definition of conditional probability, and (c) follows from the definition of the spatial Poisson distribution as well as the property of PPPs that the numbers of points in disjoint sets are independent.

As the user locations follow a homogeneous PPP with density λ, the probability that the number of users inside $\mathcal{A}_1\cap\mathcal{C}(\beta)$ is not less than m can be expressed as

$$\mathbb{P}\left(N_{\rm n}\ge m\right)=1-\sum_{j=0}^{m-1}\frac{\left(\lambda R_1^2\beta\right)^j}{2^j j!}\exp\left(-\frac{\lambda R_1^2\beta}{2}\right). \quad (45)$$

By substituting (45) into (44), we obtain $\overline{F}_{r_{{\rm n},m}}(r)$. By taking the first derivative of $F_{r_{{\rm n},m}}(r)=1-\overline{F}_{r_{{\rm n},m}}(r)$, the PDF of distance $r_{\mathrm{n},m}$ can be expressed as

$$f_{r_{\mathrm{n},m}}(r) = \frac{\frac{\beta\lambda r}{(m-1)!}\left(\frac{\beta\lambda}{2}r^2\right)^{m-1}\exp\left(-\frac{\beta\lambda}{2}r^2\right)}{1-\sum_{j=0}^{m-1}\frac{\left(\lambda R_1^2\beta\right)^j}{2^j j!}\exp\left(-\frac{\lambda R_1^2\beta}{2}\right)} = C_2 r^{2m-1}\exp\left(-\frac{\beta\lambda}{2}r^2\right), \quad 0\le r\le R_1, \tag{46}$$

where

$$C_2 = \frac{(\beta\lambda)^m \exp\left(\beta\lambda R_1^2/2\right)}{2^{m-1}(m-1)!\sum_{j=m}^{\infty}\frac{\left(\lambda\beta R_1^2\right)^j}{2^j j!}}. \tag{47}$$

Note that angle $\tau_{\mathrm{n},m}$ is uniformly distributed within $[0,\beta]$, i.e., $f_{\tau_{\mathrm{n},m}}(\tau) = 1/\beta$.

By substituting the PDFs of distance $r_{\mathrm{n},m}$ and angle $\tau_{\mathrm{n},m}$ of user $u_{\mathrm{n},m}$ with respect to base station S into (19), the probability that the m-th nearest user inside $\mathcal{A}_1\cap\mathcal{C}(\beta)$ can successfully decode both signals received from the base station after being in the listening mode for the first k blocks can be expressed as

$$\begin{aligned}
&\widetilde{D}_T(k)\\
&= \int_0^{R_1}\exp\left(-G(k)r_{\mathrm{n},m}^{\eta}\right)C_2 r_{\mathrm{n},m}^{2m-1}\exp\left(-\frac{\beta\lambda}{2}r_{\mathrm{n},m}^2\right)\mathrm{d}r_{\mathrm{n},m}\\
&\overset{(a)}{\approx} \frac{C_2R_1\pi}{2C}\sum_{c=1}^{C}\sqrt{1-\omega_c^2}\exp\left(-G(k)r_{\mathrm{n},c}^{\eta}-\frac{\beta\lambda}{2}r_{\mathrm{n},c}^2\right)\\
&\quad\times r_{\mathrm{n},c}^{2m-1},
\end{aligned} \tag{48}$$

where (a) follows by applying Gauss-Chebyshev quadrature. By substituting (48) into (22) and (23), the probability mass function of decision time $\mathcal{D}$, i.e., $\mathbb{P}(\mathcal{D}=k)$, is obtained.

B. Outage Probability of Near User

Assuming that there are at least m users inside $\mathcal{A}_1\cap\mathcal{C}(\beta)$, the outage probability of the m-th nearest user inside $\mathcal{A}_1\cap\mathcal{C}(\beta)$ is the probability that the near user fails to decode its own signal within the entire time slot. Following similar steps as in (25), the outage probability of the m-th nearest user inside $\mathcal{A}_1\cap\mathcal{C}(\beta)$ can be approximated as

$$\begin{aligned}
q_{\mathrm{out,n},m} &= 1-\widetilde{D}_T(K)\\
&\overset{(a)}{\approx} 1-\frac{C_2R_1\pi}{2C}\sum_{c=1}^{C}\sqrt{1-\omega_c^2}\,r_{\mathrm{n},c}^{2m-1}\\
&\quad\times\exp\left(-G(K)r_{\mathrm{n},c}^{\eta}-\frac{\beta\lambda}{2}r_{\mathrm{n},c}^2\right),
\end{aligned} \tag{49}$$

where (a) follows by substituting (48) with $k=K$.

For the special case $\eta=2$, a closed-form expression for $\widetilde{D}_T(k)$ can be derived. Hence, the following corollary provides the exact outage probability of the m-th nearest user inside $\mathcal{A}_1\cap\mathcal{C}(\beta)$ when the path loss exponent is 2.

Corollary 3. *For the special case of $\eta=2$, assuming that there are at least m users within $\mathcal{A}_1\cap\mathcal{C}(\beta)$, the outage probability of the m-th nearest user inside $\mathcal{A}_1\cap\mathcal{C}(\beta)$ of the DDF-based cooperative NOMA scheme with distance-based user pairing can be simplified as*

$$\begin{aligned}
q_{\mathrm{out,n},m} = 1 &- \frac{C_2}{2}\left(G(K)+\frac{\beta\lambda}{2}\right)^{-m}\\
&\times\gamma\left(m,\left(G(K)+\frac{\beta\lambda}{2}\right)R_1^2\right),
\end{aligned} \tag{50}$$

where $G(K)$ and C_2 are given in (20) and (47), respectively.

Proof. When path loss exponent $\eta=2$, the outage probability of the m-th nearest user within $\mathcal{A}_1\cap\mathcal{C}(\beta)$ is $q_{\mathrm{out,n},m} = 1-C_2\int_0^{R_1}\exp\left(-\left(G(K)+\frac{\beta\lambda}{2}\right)r_{\mathrm{n},m}^2\right)r_{\mathrm{n},m}^{2m-1}\mathrm{d}r_{\mathrm{n},m}$. By calculating the integral over distance $r_{\mathrm{n},m}$, we obtain (50). □

C. Outage Probability of Far User

Similarly, an outage event occurs at the v-th nearest user inside $\mathcal{A}_2\cap\mathcal{C}(\beta)$ when it fails to decode its own signal after the entire time slot. The general expression of the outage probability is given by (26). The following proposition provides the outage probability of the v-th nearest user inside $\mathcal{A}_2\cap\mathcal{C}(\beta)$ when pairing with the m-th nearest user inside $\mathcal{A}_1\cap\mathcal{C}(\beta)$ for the proposed DDF-based cooperative NOMA scheme.

Proposition 2. *Assuming that there are at least m users inside $\mathcal{A}_1\cap\mathcal{C}(\beta)$ and v users inside $\mathcal{A}_2\cap\mathcal{C}(\beta)$, the outage probability of the v-th nearest user inside $\mathcal{A}_2\cap\mathcal{C}(\beta)$ when pairing with the m-th nearest user inside $\mathcal{A}_1\cap\mathcal{C}(\beta)$ of DDF-based cooperative NOMA with distance-based user pairing can be approximated as in (51), shown at the top of the next page, if $\alpha_{\mathrm{f}}^2>\theta\left(R_{\mathrm{f}}^{\mathrm{th}},K\right)\alpha_{\mathrm{n}}^2$, otherwise $q_{\mathrm{out,f},v}=1$, where ψ_j, $r_{\mathrm{f},j}$, ω_c, $r_{\mathrm{n},c}$, ζ_l, $\tau_{D,l}$, J, C, and L are defined in Proposition 1, $Q_z(r_{\mathrm{f},j},r_{\mathrm{n},c},\tau_{D,l},k)$ is given in (30), $C_4=1-\widetilde{D}_T(K-1)$, and*

$$C_3 = \frac{(\beta\lambda)^v\exp\left(\beta\lambda R^2/2\right)}{2^{v-1}(v-1)!\sum_{j=v}^{\infty}(\lambda\beta)^j(R^2-R_1^2)^j/(2^j j!)}. \tag{52}$$

Proof. Please refer to Appendix C. □

The accuracy of the approximation in Proposition 2 is also verified in Section V by computer simulations. In addition to the parameters that influence the performance of random user pairing, the outage probability of the far user of DDF-based cooperative NOMA with distance-based user pairing is further dependent on the user density (λ) and the distance indices of the paired NOMA users (m and v). In particular, the outage probability in (51) decreases as the user density (λ) increases and the distance index of the far user (v) decreases, as the probability that the selected far user has a smaller path loss increases. Compared to random user pairing, distance-based user pairing can achieve a lower outage probability at the cost of generating more feedback overhead to enable the base station to acquire accurate distance information.

Following a similar analysis as for random user pairing, the diversity order for the far user of distance-based user pairing can be derived. Based on (49) and (77), when $\rho\to\infty$, we have $q_{\mathrm{out,f},v}^{\mathrm{I}}\sim 1/\rho^2$ and $q_{\mathrm{out,f},v}^{\mathrm{II}}\sim 1/\rho^3$. Thereby, the diversity

$$q_{\mathrm{out,f},v} \approx C_4 \left(1 - \frac{C_3(R-R_1)\pi}{2J} \sum_{j=1}^{J} \sqrt{1-\psi_j^2}\, r_{\mathrm{f},j} \left(r_{\mathrm{f},j}^2 - R_1^2\right)^{v-1} \exp\left(-C_1 r_{\mathrm{f},j}^{\eta} - \frac{\beta\lambda}{2} r_{\mathrm{f},j}^2\right)\right)$$
$$+ \frac{R_1(R-R_1)C_2C_3\pi^3}{4CLJ\beta} \sum_{c=1}^{C} \sqrt{1-\omega_c^2} \sum_{l=1}^{L} \sqrt{1-\zeta_l^2} \sum_{j=1}^{J} \sqrt{1-\psi_j^2} \sum_{k=1}^{K-1} Q_n(r_{\mathrm{n},c},k)$$
$$\times Q_z(r_{\mathrm{f},j}, r_{\mathrm{n},c}, \tau_{D,l}, k) r_{\mathrm{f},j}^{\eta+1} \left(r_{\mathrm{f},j}^2 - R_1^2\right)^{v-1} r_{\mathrm{n},c}^{2m-1}(\beta - \tau_{D,l}) \exp\left(-\frac{\beta\lambda}{2}\left(r_{\mathrm{f},j}^2 + r_{\mathrm{n},c}^2\right)\right), \quad (51)$$

order for the v-th nearest user $u_{\mathrm{f},v}$ is 2, which is independent of the distance index of the far user (v). Hence, comparing with (38), random and distance-based user pairing achieve the same diversity order for the far user. This is due to the fact that, the considered user pairing strategy exploits distance information but not instantaneous CSI, which would be needed to increase the diversity order. Similarly, the diversity order for the near user is one, regardless of the distance index of the near user (m).

D. Sum Rate

Based on the analysis of the outage probabilities of the near and the far users (i.e., $u_{\mathrm{n},m}$ and $u_{\mathrm{f},v}$), the sum rate of the m-th nearest user inside $\mathcal{C}(\beta) \cap \mathcal{A}_1$ and the v-th nearest user inside $\mathcal{C}(\beta) \cap \mathcal{A}_2$ of DDF-based cooperative NOMA with distance-based user pairing is given by

$$R_{\mathrm{sum},m,v} = (1 - q_{\mathrm{out,n},m}) R_{\mathrm{n}}^{\mathrm{th}} + (1 - q_{\mathrm{out,f},v}) R_{\mathrm{f}}^{\mathrm{th}}, \quad (53)$$

where $q_{\mathrm{out,n},m}$ and $q_{\mathrm{out,f},v}$ are given in (49) and (51), respectively.

V. Performance Evaluation

In this section, we present simulation and analytical results for the proposed DDF-based cooperative NOMA scheme and compare them with corresponding results for conventional NOMA [12], cooperative NOMA [17], and OMA. For conventional NOMA, the base station transmits the superimposed mixture of the near and the far users' signals during the entire time slot. For cooperative NOMA, the base station transmits to the near and the far users in the first half of a time slot using NOMA, and the near user acts as a relay in the second half of the time slot if it can successfully decode the signal intended for the far user. Hence, the spectral efficiency of cooperative NOMA is reduced by half. At the end of the time slot, the far user uses maximum ratio combining (MRC) to decode the signals received from the base station and the near user. For OMA, the base station transmits the signals to the near and the far users in the first and second half of a time slot, respectively. In the simulations, we consider a circular network coverage area with radius $R = 800$ m. The noise power and the path loss exponent are set to -100 dBm and 3.8, respectively. We assume Rayleigh fading channels. Unless specified otherwise, we set $K = 20$, $R_1 = 300$ m, $P_S = P_U$, $\alpha_{\mathrm{f}}^2 = 0.8$, $\alpha_{\mathrm{n}}^2 = 0.2$, $\beta = \pi/3$, and $\lambda = 5 \times 10^{-5}$ nodes/m^2. In addition, we set $C = I = J = L = 30$, which are sufficiently large values to guarantee the accuracy of the approximation.

Fig. 2 illustrates the impact of the transmit power on the outage probabilities of the near and the far users of DDF-based cooperative NOMA with random user pairing as given in (25) and (29), respectively. The simulation results are in good agreement with the analytical (A) results, which validates the performance analysis. For DDF-based cooperative NOMA, the outage probability of the far user is lower than that of the near user when the transmit power is larger than 17 dBm. This is because the outage probability of the far user decreases faster than that of the near user by exploiting cooperative diversity. The outage probabilities of the near and the far users of DDF-based cooperative NOMA are lower than those of cooperative NOMA, because cooperative NOMA reduces the spectral efficiency by half to achieve cooperative diversity. For the far user, DDF-based cooperative NOMA always achieves a lower outage probability than conventional NOMA because of the cooperative diversity. On the other hand, DDF-based cooperative NOMA and conventional NOMA achieve the same outage probability for the near user. This is because for both schemes, an outage event occurs if and only if the near user cannot successfully decode its signal received from the base station by the end of the time slot. In addition, the slopes of the outage probabilities of the far user are identical for cooperative NOMA and DDF-based cooperative NOMA, which confirms that they achieve the same diversity order.

Fig. 3 shows the impact of the far user's target data rate (i.e., $R_{\mathrm{f}}^{\mathrm{th}}$) on the outage probability for different NOMA schemes with random user pairing. To successfully decode the signal for a higher target data rate, a higher reception threshold in terms of the SINR is required at the receiver. Therefore, the outage probability increases with $R_{\mathrm{f}}^{\mathrm{th}}$ for all schemes. Cooperative NOMA outperforms conventional NOMA when $R_{\mathrm{f}}^{\mathrm{th}}$ is small as the far user exploits cooperative diversity. However, when $R_{\mathrm{f}}^{\mathrm{th}} \geq 1.25$ BPCU, the far user is always in outage for cooperative NOMA because of the loss in spectral efficiency incurred by cooperation. In contrast, the proposed DDF-based cooperative NOMA scheme achieves cooperative diversity without sacrificing spectral efficiency. Hence, the outage probability of the far user is always lower for DDF-based cooperative NOMA than for conventional NOMA and cooperative NOMA. In fact, the proposed DDF-based cooperative NOMA scheme adapts to the instantaneous channel conditions and dynamically decides when the near user should switch from the listening mode to the transmit mode. On the other hand, the probability that either the near user or the far user is in outage is the complement of the probability that

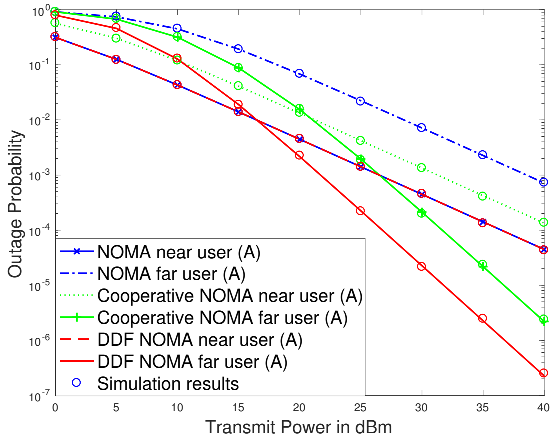

Fig. 2: Outage probabilities of the near and the far users versus the transmit power for $R_{\rm f}^{\rm th}=R_{\rm n}^{\rm th}=1$ bit per channel use (BPCU).

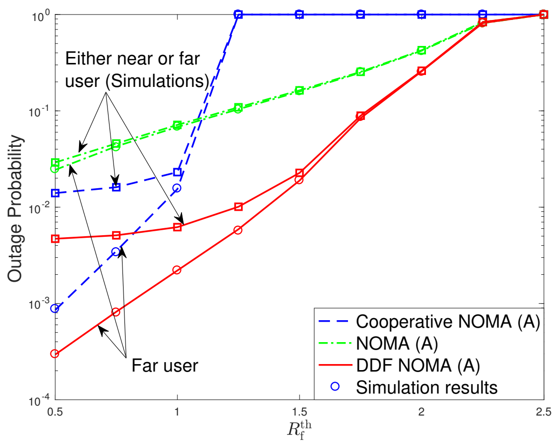

Fig. 3: Outage probability versus far user's target data rate $R_{\rm f}^{\rm th}$ for $P_S=20$ dBm and $R_{\rm n}^{\rm th}=1$ BPCU.

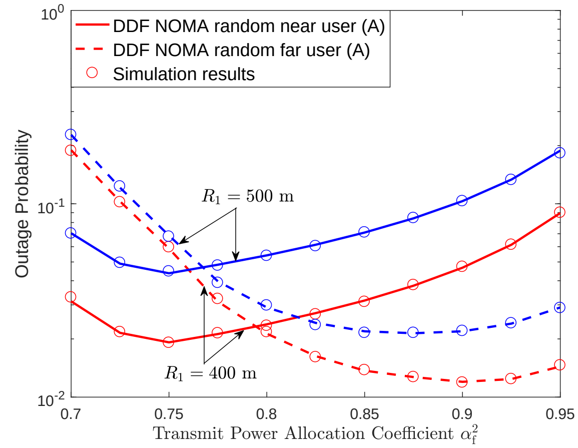

Fig. 4: Outage probability versus transmit power allocation coefficient $\alpha_{\rm f}^2$ for different values of R_1 when $R_{\rm f}^{\rm th}=R_{\rm n}^{\rm th}=1.5$ BPCU and $P_S=20$ dBm.

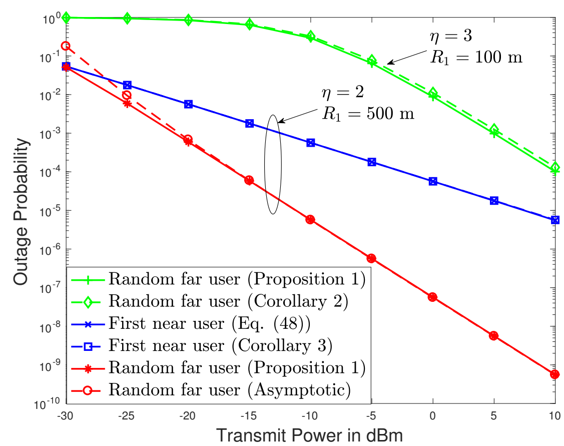

Fig. 5: Outage probability versus transmit power for $R_{\rm f}^{\rm th}=1.5$ BPCU and $R_{\rm n}^{\rm th}=2$ BPCU.

both users can successfully decode their own signals. For all considered NOMA schemes, the probability that either the near user or the far user is in outage is dominated by the outage probability of the near user when $R_{\rm f}^{\rm th}$ is small, and is equal to the outage probability of the far user when $R_{\rm f}^{\rm th}$ is large.

Fig. 4 shows the impact of the transmit power allocation coefficients (i.e., $\alpha_{\rm f}^2$) and the radius of the inner circle (i.e., R_1) on the outage probabilities of DDF-based cooperative NOMA with random user pairing. By increasing $\alpha_{\rm f}^2$ from 0.7 to 0.75, the outage probability of the near user decreases, as the near user has a higher probability to successfully perform SIC. However, by increasing $\alpha_{\rm f}^2$ further, the outage probability of the near user increases. This is because the benefits introduced by increasing the probability of successful SIC cannot compensate the reduction of the SNR of the signal intended for the near user. By increasing $\alpha_{\rm f}^2$ from 0.9 to 0.95, the outage probability of the far user increases. This is because the probability that the near user successfully decodes the signal intended for the far user decreases, which in turn reduces the probability that the near user can assist the transmission of the far user. Overall, the near and the far users achieve the lowest outage probabilities at different values of $\alpha_{\rm f}^2$, and the value of $\alpha_{\rm f}^2$ can be set to balance the performances of the near and the far users. By increasing R_1 from 400 m to 500 m, the outage probabilities of both near and far users increase, as both users are more likely to suffer from a larger path loss. Due to its higher diversity gain, the performance degradation of the far user when increasing R_1 is less significant than that of the near user.

Fig. 5 plots the outage probabilities of the near and the far users of DDF-based cooperative NOMA for three special cases. For path loss exponent $\eta=2$, the outage probability of a randomly selected far user, given in (29), can asymptotically be simplified as in (34). As we can see, the asymptotic results are in good agreement with the analytical results, especially when the transmit power exceeds -20 dBm. Fig. 5 validates the approximate and exact outage probabilities of the first near user when $\eta=2$, given in (49) and (50), respectively. Moreover, the approximation of $\left(r_{\rm f}^2+r_{\rm n}^2-2r_{\rm f}r_{\rm n}\cos\tau_D\right)^{\eta/2}\approx r_{\rm f}^{\eta}$ is more accurate when the value of R_1 is smaller. As we can see, the approximate expression given in Corollary 2 is accurate when $R_1=100$ m. Note that the outage probability of the far user derived in Proposition 1 is accurate for any value of R_1.

Fig. 6 shows the impact of the user density (i.e., λ) on the outage probabilities of the near and the far users for the proposed DDF-based cooperative NOMA scheme with distance-based user pairing. If the near and the far users closest to the base station, i.e., $(m, v) = (1, 1)$, are paired, the outage probabilities of the near and the far users are lower than those for randomly selected near and far users, respectively. This is because the nearest users suffer from the same or a smaller path loss than randomly selected users. By increasing (m, v) from $(1, 1)$ to $(2, 2)$, the outage probabilities of both the near and the far users increase due to the increased path loss, which illustrates the impact of the users' locations on the network performance. In the low user density region, random user pairing outperforms distance-based user pairing with $(m, v) = (2, 2)$. As the user density increases, the outage probability for distance-based user pairing decreases, as the probability of selecting a user closer to the base station increases. However, the outage probability of random user pairing does not depend on the user density. As a result, for high user densities, distance-based user pairing achieves lower outage probabilities than random user pairing for both the near and the far users.

In Fig. 7, we study the impact of the transmit power and the far user's target data rate on the sum rates of different NOMA schemes with random user pairing. When $R_{\mathrm{f}}^{\mathrm{th}} = 1$ BPCU, as the transmit power increases, the sum rates of all NOMA schemes increase, as the probability of successful signal reception at each user increases. Cooperative NOMA achieves a lower sum rate than conventional NOMA when the transmit power is smaller than 8 dBm. This is because lower transmit powers lead to a lower probability of successful signal reception at the near user, which in turn reduces the probability that cooperative transmission is possible. Thereby, the achieved cooperation gain cannot compensate for the loss in spectral efficiency. However, when the transmit power is higher than 8 dBm, cooperative NOMA outperforms conventional NOMA. As it can exploit the benefits of cooperative transmission without sacrificing spectral efficiency, the proposed DDF-based cooperative NOMA scheme always achieves a higher sum rate than conventional NOMA and cooperative NOMA. On the other hand, when $R_{\mathrm{f}}^{\mathrm{th}}$ is increased from 1 BPCU to 2 BPCU, the sum rate of DDF-based cooperative NOMA becomes smaller for transmit powers smaller than 16 dBm, due to the relative increase in the outage probability. When $R_{\mathrm{f}}^{\mathrm{th}} = 2$ BPCU, the sum rate of cooperative NOMA is always 0, as the condition $\alpha_{\mathrm{f}}^2 > \theta\left(2R_{\mathrm{f}}^{\mathrm{th}}, K\right)\alpha_{\mathrm{n}}^2$ needed for successful decoding cannot be satisfied regardless of the value of the transmit power.

In Fig. 8, the sum rates of DDF-based cooperative NOMA with distance-based user pairing and OMA are shown for different choices of the near user's target data rate. DDF-based cooperative NOMA achieves a higher sum rate than OMA in all considered cases. When $(m, v) = (1, 1)$, the performance gain of DDF-based cooperative NOMA over OMA is enlarged by increasing $R_{\mathrm{n}}^{\mathrm{th}}$ from 2 BPCU to 4 BPCU. This is because the adverse effect of the low spectral efficiency of OMA becomes more pronounced for larger $R_{\mathrm{n}}^{\mathrm{th}}$. Hence, it is more

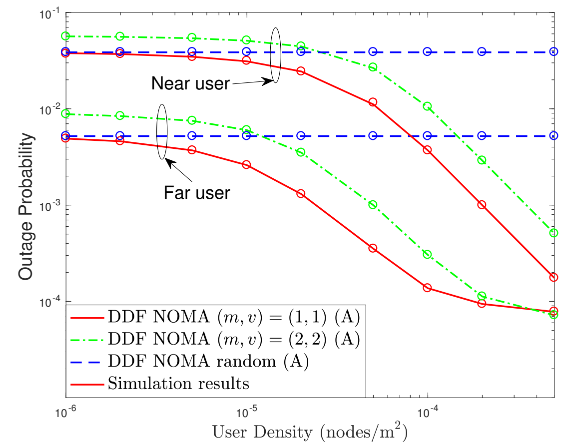

Fig. 6: Outage probability versus user density when $R_1 = 400$ m, $P_S = 20$ dBm, $R_{\mathrm{f}}^{\mathrm{th}} = 1$ BPCU, and $R_{\mathrm{n}}^{\mathrm{th}} = 2$ BPCU.

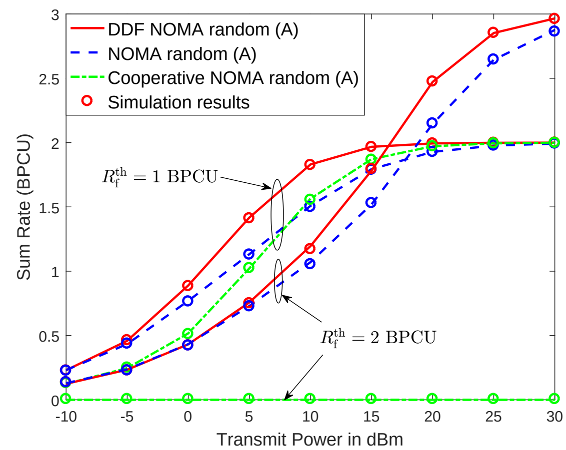

Fig. 7: Sum rate versus transmit power for different values of $R_{\mathrm{f}}^{\mathrm{th}}$ when $R_{\mathrm{n}}^{\mathrm{th}} = 1$ BPCU.

desirable to pair near and far users with more diverse target data rates. On the other hand, by increasing v from 1 to 8 for $R_{\mathrm{n}}^{\mathrm{th}} = 2$ BPCU, the sum rate of DDF-based cooperative NOMA decreases due to the larger associated path loss. When the transmit SNR exceeds 30 dBm, the sum rate converges to the summation of the target data rates of both users, as the received SINR at each user is large enough to guarantee successful signal reception.

Fig. 9 illustrates the impact of the user density (i.e., λ) and the near user's target data rate on the sum rates of DDF-based cooperative NOMA with random and distance-based user pairing. As the user density increases, the sum rate of distance-based user pairing increases, because the probability of selecting a user closer to the base station increases. However, the sum rate of random user pairing does not depend on the user density, as the distribution of the locations of randomly selected users does not change. Due to the smaller associated path loss, distance-based user pairing outperforms random user pairing for $(m, v) = (1, 1)$ and for $(m, v) = (2, 2)$ when $\lambda > 9 \times 10^{-4}$ nodes/m^2. Furthermore, when $R_{\mathrm{n}}^{\mathrm{th}}$ is increased from 2 BPCU to 3 BPCU, the performance gain of distance-based user pairing over random user pairing becomes

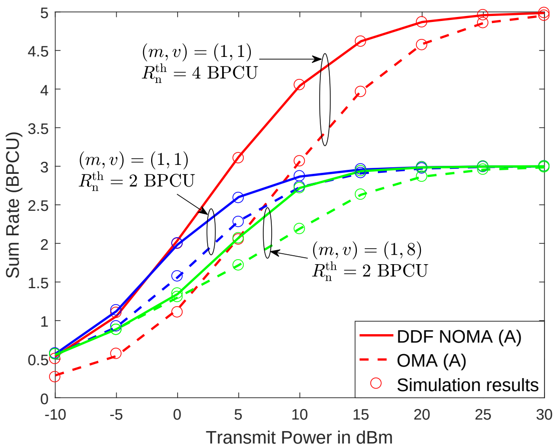

Fig. 8: Sum rate versus transmit power for different values of $R_{\rm n}^{\rm th}$ when $R_{\rm f}^{\rm th}=1$ BPCU.

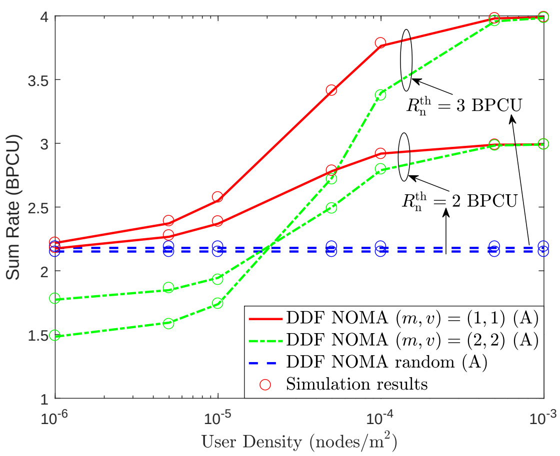

Fig. 9: Sum rate versus user density for different values of $R_{\rm n}^{\rm th}$ when $P_S=10$ dBm, $R_1=400$ m, and $R_{\rm f}^{\rm th}=1$ BPCU.

larger, which again indicates that a larger sum rate gain can be achieved when users having more diverse target data rates are paired. When the node density exceeds 10^{-3} nodes/m^2, distance-based user pairing achieves the highest sum rate gain over random user pairing, as the selected users are close to the base station and can always successfully decode the signals.

Based on the presented numerical results, in Table I, we summarize the impact of important system parameters on the performance of the proposed DDF-based cooperative NOMA scheme.

VI. Conclusions

In this paper, we proposed a DDF-based cooperative NOMA scheme for downlink transmission with spatially random users. We investigated random and distance-based user pairing strategies, which require one-bit feedback and the users' distance information at the base station, respectively. Tools from stochastic geometry were utilized to derive analytical expressions for the outage probabilities of the near and the far users, the diversity order, and the sum rate of the proposed scheme. Simulation results validated the performance analysis and showed that the proposed DDF-based cooperative NOMA scheme outperforms OMA, conventional NOMA, and cooperative NOMA. In contrast to these competing schemes, DDF-based cooperative NOMA achieves cooperative diversity for superposition transmission without sacrificing spectral efficiency. Our results revealed that the sum rate gain of DDF-based cooperative NOMA over OMA is higher when NOMA users with more diverse target data rates are paired, and the performance gain of distance-based user pairing over random user pairing increases with the user density.

TABLE I: Impact of Important System Parameters.

Parameter	Impact
Target data rates ($R_{\rm f}^{\rm th}$ and $R_{\rm n}^{\rm th}$)	The sum rate gain of DDF-based cooperative NOMA over OMA increases with the gap between $R_{\rm n}^{\rm th}$ and $R_{\rm f}^{\rm th}$.
User density (λ)	The performance (i.e., outage probability and sum rate) gain of distance-based user pairing over random user pairing increases with λ.
Transmit power (P_S)	The outage probability of the far user decreases faster with increasing transmit power than that of the near user.
Power allocation coefficient ($\alpha_{\rm f}^2$)	There exist optimal values of $\alpha_{\rm f}^2$ which minimize the outage probabilities of the near and the far users, respectively.
User distance indices (m and v)	The performance gain of distance-based user pairing over random user pairing decreases with m and v.

Appendix

A. Proof of Proposition 1

Based on (26), the probability that Case I occurs is given by

$$q_{\rm out,f}^{\rm I} \overset{(a)}{=} \mathbb{P}\left(\mathcal{D}=K\right)\mathbb{P}\left(\frac{\alpha_{\rm f}^2 P_S|h_{\rm f}|^2\ell(x_{\rm f})}{\alpha_{\rm n}^2 P_S|h_{\rm f}|^2\ell(x_{\rm f})+\sigma^2}<\theta(R_{\rm f}^{\rm th},K)\right)$$
$$=\left(1-D_T(K-1)\right)\mathbb{E}_{x_{\rm f}}\left(1-\exp\left(-C_1 r_{\rm f}^{\eta}\right)\right), \qquad (54)$$

where (a) follows from the independent channel fading assumption across different links.

For random user pairing, the PDFs of distance $r_{\rm f}$ and angle $\tau_{\rm f}$ of far user $u_{\rm f}$ with respect to base station S are $f_{r_{\rm f}}(r)=2r/(R^2-R_1^2)$ and $f_{\tau_{\rm f}}(\tau)=1/\beta$, respectively. Thus, we have

$$q_{\rm out,f}^{\rm I}=\left(1-D_T(K-1)\right)$$
$$\times\left(1-\int_0^{\beta}\int_{R_1}^{R}\exp\left(-C_1 r_{\rm f}^{\eta}\right)\frac{2r_{\rm f}}{R^2-R_1^2}{\rm d}r_{\rm f}\frac{1}{\beta}{\rm d}\tau_{\rm f}\right)$$
$$=\left(1-D_T(K-1)\right)$$
$$\times\left(1-\frac{2}{\eta\left(R^2-R_1^2\right)}C_1^{-2/\eta}\right.$$
$$\left.\times\left(\gamma\left(\frac{2}{\eta},C_1R^{\eta}\right)-\gamma\left(\frac{2}{\eta},C_1R_1^{\eta}\right)\right)\right). \qquad (55)$$

The SINRs of signal $\{s_{{\rm f},i}\}$ observed at the far user $u_{\rm f}$ in the first and second phases are correlated as the value of $|h_{\rm f}|^2$ does not change throughout the time slot. To facilitate the calculation of the probability that Case II occurs, we denote the achievable rate at the far user $u_{\rm f}$ in the first phase by

$Z = \frac{k}{K}\log_2\left(1+\Gamma^{\mathrm{I}}_{\mathrm{f|n}}\right)$. The cumulative distribution function (CDF) of random variable Z is given by

$$\begin{aligned} F_Z(z) &= \mathbb{P}\left(\frac{k}{K}\log_2\left(1+\Gamma^{\mathrm{I}}_{\mathrm{f|n}}\right) \le z\right) \\ &\overset{(a)}{=} \mathbb{P}\left(|h_{\mathrm{f}}|^2 \le \frac{\theta(z,k)\sigma^2 r_{\mathrm{f}}^{\eta}}{\left(\alpha_{\mathrm{f}}^2-\theta(z,k)\alpha_{\mathrm{n}}^2\right)P_S}\right) \\ &= 1-\exp\left(-\frac{\theta(z,k)\sigma^2 r_{\mathrm{f}}^{\eta}}{\left(\alpha_{\mathrm{f}}^2-\theta(z,k)\alpha_{\mathrm{n}}^2\right)P_S}\right), \end{aligned} \tag{56}$$

if $\alpha_{\mathrm{f}}^2 > \theta(z,k)\alpha_{\mathrm{n}}^2$, where (a) follows by substituting (5).

The condition for the existence of the CDF of random variable Z, i.e., $\alpha_{\mathrm{f}}^2 > \theta(Z,k)\alpha_{\mathrm{n}}^2$, can be equivalently expressed as

$$Z < \frac{k}{K}\log_2\left(1+\frac{\alpha_{\mathrm{f}}^2}{\alpha_{\mathrm{n}}^2}\right). \tag{57}$$

By taking the first derivative of $F_Z(z)$, the PDF of random variable Z can be expressed as

$$\begin{aligned} f_Z(z) &= \frac{\mathrm{d}}{\mathrm{d}z}F_Z(z) \\ &= \exp\left(-\frac{\sigma^2\theta(z,k)r_{\mathrm{f}}^{\eta}}{\left(\alpha_{\mathrm{f}}^2-\theta(z,k)\alpha_{\mathrm{n}}^2\right)P_S}\right) \\ &\quad\times\frac{\alpha_{\mathrm{f}}^2\sigma^2\left(\theta(z,k)+1\right)r_{\mathrm{f}}^{\eta}K\ln 2}{\left(\alpha_{\mathrm{f}}^2-\theta(z,k)\alpha_{\mathrm{n}}^2\right)^2 P_S k} \\ &= \exp\left(-G_1(z,k)r_{\mathrm{f}}^{\eta}\right)G_2(z,k)r_{\mathrm{f}}^{\eta}, \end{aligned} \tag{58}$$

where $G_1(z,k)$ and $G_2(z,k)$ are defined in (31) and (32), respectively.

Based on (28), for a given decision time k, we obtain (59), shown at the top of the next page, where (a) follows by substituting (17) and (b) is due to the Rayleigh fading channel.

Based on the definition of Z, we have $P_S h_{\mathrm{f}}^2\ell(x_{\mathrm{f}}) = \theta(Z,k)\sigma^2/\left(\alpha_{\mathrm{f}}^2-\theta(Z,k)\alpha_{\mathrm{n}}^2\right)$. By substituting it into (59), $Q(k)$ can be simplified as

$$\begin{aligned} &Q(k) \\ &= \mathbb{E}_Z\left(1-\exp\left(-\frac{\sigma^2\alpha_{\mathrm{f}}^2\left(\theta\left(R_{\mathrm{f}}^{\mathrm{th}}-Z,K-k\right)-\theta\left(Z,k\right)\right)}{\left(\alpha_{\mathrm{f}}^2-\theta(Z,k)\alpha_{\mathrm{n}}^2\right)P_U\ell(x_{\mathrm{f}}-x_{\mathrm{n}})}\right)\right) \\ &= \mathbb{E}_Z\left(1-\exp\left(-\frac{G_3(Z,k)}{\ell(x_{\mathrm{f}}-x_{\mathrm{n}})}\right)\right), \end{aligned}$$

where $G_3(Z,k)$ is defined in (33).

As $Q(k)$ can be interpreted as the probability that the far user u_{f} fails to decode signal $\{s_{\mathrm{f},i}\}$ received from base station S for decision time $\mathcal{D}=k$, the value of $Q(k)$ should be greater than or equal to 0. To ensure $Q(k)\ge 0$, we have $\theta\left(R_{\mathrm{f}}^{\mathrm{th}}-Z,K-k\right)\ge\theta\left(Z,k\right)$, which is equivalent to

$$Z \le \frac{k}{K}R_{\mathrm{f}}^{\mathrm{th}}. \tag{60}$$

We set $R_{\mathrm{f}}^{\mathrm{th}} < \log_2(1+\frac{\alpha_{\mathrm{f}}^2}{\alpha_{\mathrm{n}}^2})$, which leads to $Z \le \frac{k}{K}R_{\mathrm{f}}^{\mathrm{th}}$ based on (57) and (60). Otherwise, if $R_{\mathrm{f}}^{\mathrm{th}} \ge \log_2(1+\frac{\alpha_{\mathrm{f}}^2}{\alpha_{\mathrm{n}}^2})$, the far user u_{f} is always in outage (i.e., $q_{\mathrm{out,f}}=1$), regardless of the channel condition between base station S and the far user u_{f}.

By taking into account the constraint on Z, $Q(k)$ is given by

$$\begin{aligned} Q(k) &= \int_0^{\frac{k}{K}R_{\mathrm{f}}^{\mathrm{th}}}\left(1-\exp\left(-\frac{G_3(z,k)}{\ell(x_{\mathrm{f}}-x_{\mathrm{n}})}\right)\right)f_Z(z)\mathrm{d}z \\ &\overset{(a)}{=} \int_0^{\frac{k}{K}R_{\mathrm{f}}^{\mathrm{th}}}\left(1-\exp\left(-\frac{G_3(z,k)}{\ell(x_{\mathrm{f}}-x_{\mathrm{n}})}\right)\right) \\ &\quad\times\exp\left(-G_1(z,k)r_{\mathrm{f}}^{\eta}\right)G_2(z,k)r_{\mathrm{f}}^{\eta}\mathrm{d}z, \end{aligned} \tag{61}$$

where (a) follows by substituting (58), $\ell(x_{\mathrm{f}}-x_{\mathrm{n}}) = \left(r_{\mathrm{f}}^2+r_{\mathrm{n}}^2-2r_{\mathrm{f}}r_{\mathrm{n}}\cos\tau_D\right)^{-\eta/2}$, and $\tau_D = |\tau_{\mathrm{f}}-\tau_{\mathrm{n}}|$ denotes the absolute value of the angle difference between angles τ_{f} and τ_{n}.

Based on the above analysis, the probability that Case II occurs can be expressed as

$$\begin{aligned} q_{\mathrm{out,f}}^{\mathrm{II}} = \mathbb{E}_{x_{\mathrm{n}},x_{\mathrm{f}}}\Bigg(&\sum_{k=1}^{K-1}Q_n(r_{\mathrm{n}},k)\int_0^{\frac{k}{K}R_{\mathrm{f}}^{\mathrm{th}}}\left(1-\exp\left(-\frac{G_3(z,k)}{\ell(x_{\mathrm{f}}-x_{\mathrm{n}})}\right)\right) \\ &\times\exp\left(-G_1(z,k)r_{\mathrm{f}}^{\eta}\right)G_2(z,k)r_{\mathrm{f}}^{\eta}\mathrm{d}z\Bigg), \end{aligned} \tag{62}$$

where $Q_n(r_{\mathrm{n}},k)$ is defined in (27).

As angles τ_{f} and τ_{n} are uniformly distributed within $[0,\beta]$ and independent from each other, the CDF of $\tau_D = |\tau_{\mathrm{f}}-\tau_{\mathrm{n}}|$ can be expressed as $F_{\tau_D}(\tau) = \left(2\beta\tau-\tau^2\right)/\beta^2, \tau\in[0,\beta]$. By taking the first derivative of $F_{\tau_D}(\tau)$, the PDF of τ_D is given by

$$f_{\tau_D}(\tau) = \frac{\mathrm{d}}{\mathrm{d}\tau}F_{\tau_D}(\tau) = \frac{2\beta-2\tau}{\beta^2}, \quad \tau\in[0,\beta]. \tag{63}$$

By substituting the PDFs of r_{f}, r_{n}, and τ_D into (62), we have

$$\begin{aligned} q_{\mathrm{out,f}}^{\mathrm{II}} = &\frac{8}{(R^2-R_1^2)R_1^2\beta^2}\int_0^{R_1}\int_0^{\beta}\int_{R_1}^{R}\sum_{k=1}^{K-1}Q_n(r_{\mathrm{n}},k) \\ &\times Q_z(r_{\mathrm{f}},r_{\mathrm{n}},\tau_D,k)r_{\mathrm{f}}^{\eta+1}(\beta-\tau_D)r_{\mathrm{n}}\mathrm{d}r_{\mathrm{f}}\mathrm{d}\tau_D\mathrm{d}r_{\mathrm{n}}, \end{aligned} \tag{64}$$

where

$$\begin{aligned} &Q_z(r_{\mathrm{f}},r_{\mathrm{n}},\tau_D,k) = \int_0^{\frac{k}{K}R_{\mathrm{f}}^{\mathrm{th}}}\exp\left(-G_1(z,k)r_{\mathrm{f}}^{\eta}\right)G_2(z,k) \\ &\times\left(1-\exp\left(-G_3(z,k)\left(r_{\mathrm{f}}^2+r_{\mathrm{n}}^2-2r_{\mathrm{f}}r_{\mathrm{n}}\cos\tau_D\right)^{\eta/2}\right)\right)\mathrm{d}z. \end{aligned} \tag{65}$$

The direct calculation of (64) can be very involved due to multiple integrals. In the following, we approximate the integrals in (64) with summations to reduce the computational complexity by using Gauss-Chebyshev quadrature [31]. As a result, (65) can be approximated as (30). With respect to the integral over distance r_{f}, we have

$$\begin{aligned} &\int_{R_1}^{R}Q_z(r_{\mathrm{f}},r_{\mathrm{n}},\tau_D,k)r_{\mathrm{f}}^{\eta+1}\mathrm{d}r_{\mathrm{f}} \\ &\approx\frac{(R-R_1)\pi}{2J}\sum_{j=1}^{J}\sqrt{1-\psi_j^2}Q_z(r_{\mathrm{f},j},r_{\mathrm{n}},\tau_D,k)r_{\mathrm{f},j}^{\eta+1}, \end{aligned} \tag{66}$$

where J, ψ_j, and $r_{\mathrm{f},j}$ are defined in Proposition 1. For the integral over angle τ_D, we have

$$Q_\tau(r_{\mathrm{n}},k) = \int_0^{\beta}\int_{R_1}^{R}Q_z(r_{\mathrm{f}},r_{\mathrm{n}},\tau_D,k)r_{\mathrm{f}}^{\eta+1}(\beta-\tau_D)\mathrm{d}r_{\mathrm{f}}\mathrm{d}\tau_D$$

$$
\begin{aligned}
Q(k) &= \mathbb{E}_Z\left(\mathbb{P}\left(\frac{K-k}{K}\log_2\left(1+\Gamma_{\mathrm{f|n}}^{\mathrm{II}}\right) < R_{\mathrm{f}}^{\mathrm{th}} - Z \,\Big|\, Z\right)\right) \\
&\overset{(a)}{=} \mathbb{E}_Z\big(\mathbb{P}\left(P_U|h_{\mathrm{f,n}}|^2\ell(x_{\mathrm{f}}-x_{\mathrm{n}}) < \left(\alpha_{\mathrm{n}}^2 P_S|h_{\mathrm{f}}|^2\ell(x_{\mathrm{f}})+\sigma^2\right)\theta(R_{\mathrm{f}}^{\mathrm{th}}-Z,K-k)-\alpha_{\mathrm{f}}^2 P_S|h_{\mathrm{f}}|^2\ell(x_{\mathrm{f}})\,|Z\right)\big) \\
&\overset{(b)}{=} \mathbb{E}_Z\left(1-\exp\left(-\frac{\left(\alpha_{\mathrm{n}}^2 P_S|h_{\mathrm{f}}|^2\ell(x_{\mathrm{f}})+\sigma^2\right)\theta(R_{\mathrm{f}}^{\mathrm{th}}-Z,K-k)-\alpha_{\mathrm{f}}^2 P_S|h_{\mathrm{f}}|^2\ell(x_{\mathrm{f}})}{P_U\ell(x_{\mathrm{f}}-x_{\mathrm{n}})}\right)\right), \qquad (59)
\end{aligned}
$$

$$
\begin{aligned}
&= \frac{\beta\pi}{2L}\sum_{l=1}^{L}\sqrt{1-\zeta_l^2}\,\frac{(R-R_1)\pi}{2J}\sum_{j=1}^{J}\sqrt{1-\psi_j^2} \\
&\qquad \times Q_z(r_{\mathrm{f},j},r_{\mathrm{n}},\tau_{D,l},k)\,r_{\mathrm{f},j}^{\eta+1}(\beta-\tau_{D,l}), \qquad (67)
\end{aligned}
$$

where L, ζ_l, and $\tau_{D,l}$ are defined in Proposition 1.

Finally, with respect to the integral over distance r_{n}, we have

$$
\begin{aligned}
q_{\mathrm{out,f}}^{\mathrm{II}} &= \frac{4\pi}{(R^2-R_1^2)R_1\beta^2 C}\sum_{c=1}^{C}\sqrt{1-\omega_c^2} \\
&\qquad \times\left(\sum_{k=1}^{K-1}Q_n(r_{\mathrm{n},c},k)Q_\tau(r_{\mathrm{n},c},k)r_{\mathrm{n},c}\right), \qquad (68)
\end{aligned}
$$

where C, ω_c, and $r_{\mathrm{n},c}$ are defined in Proposition 1, and $Q_n(r_{\mathrm{n},c},k)$ and $Q_\tau(r_{\mathrm{n}},k)$ are given in (27) and (67), respectively.

After some algebraic manipulations and substituting (35) and (68) into (26), we obtain the outage probability of the far user of DDF-based cooperative NOMA with random user pairing, given in (29). Hence, the proof of the proposition is complete.

B. Proof of Corollary 1

When the transmit SNR is high and $k \le k_{\max}$, we have

$$
\begin{aligned}
&Q_z(r_{\mathrm{f}},r_{\mathrm{n}},\tau_D,k) \\
&\overset{(a)}{\approx} \int_0^{\frac{k}{K}R_{\mathrm{f}}^{\mathrm{th}}} G_3(z,k)\left(r_{\mathrm{f}}^2+r_{\mathrm{n}}^2-2r_{\mathrm{f}}r_{\mathrm{n}}\cos\tau_D\right)^{\frac{\eta}{2}} \\
&\qquad \times\left(1-G_1(z,k)r_{\mathrm{f}}^2\right)G_2(z,k)\mathrm{d}z, \qquad (69) \\
&\exp\left(-G(k)r_{\mathrm{n}}^{\eta}\right)-\exp\left(-G(k-1)r_{\mathrm{n}}^{\eta}\right) \\
&\overset{(b)}{\approx} \begin{cases}\left(G(k-1)-G(k)\right)r_{\mathrm{n}}^{\eta}, & \text{if } k\ge k_{\min}+1,\\ 1-G(k)r_{\mathrm{n}}^{\eta}, & \text{if } k=k_{\min},\end{cases} \qquad (70)
\end{aligned}
$$

where (a) and (b) follow by applying $\exp(-x)\approx 1-x$ when $x\to 0$.

When $\beta \le \pi/3$, by applying the small-angle approximation, we have

$$
\cos\tau_D \approx 1-\tau_D^2/2, \qquad 0\le\tau_D\le\beta. \qquad (71)
$$

By setting $\eta = 2$, substituting (69), (70), and (71) into (64), and calculating the integrals over τ_D, r_{f}, and r_{n} in sequence, we obtain (72), shown at the top of the next page, where $G_2(z,k)$ and $G_3(z,k)$ are defined in (32) and (33), respectively, and $A_4(z,k)$ and $A_5(z,k)$ are defined in Corollary 1. By using the Gauss-Chebyshev quadrature, we can obtain the outage probability of the far user, given in (34). Hence, the proof of the corollary is complete.

C. Proof of Proposition 2

Following the same steps as in (44) and (46), and assuming that there are at least v users in $\mathcal{A}_2\cap\mathcal{C}(\beta)$, the PDF of distance $r_{\mathrm{f},v}$ of user $u_{\mathrm{f},v}$ with respect to base station S can be written as

$$
\begin{aligned}
f_{r_{\mathrm{f},v}}(r) &= \frac{\beta\lambda r}{(v-1)!\mathbb{P}(N_{\mathrm{f}}\ge v)}\left(\frac{\beta\lambda}{2}\left(r^2-R_1^2\right)\right)^{v-1} \\
&\qquad \times\exp\left(-\frac{\beta\lambda}{2}\left(r^2-R_1^2\right)\right) \\
&= C_3 r\left(r^2-R_1^2\right)^{v-1}\exp\left(-\beta\lambda r^2/2\right), \qquad (73)
\end{aligned}
$$

where $R_1\le r\le R$, C_3 is given in (52), and

$$
\begin{aligned}
&\mathbb{P}\left(N_{\mathrm{f}}\ge v\right) \\
&= 1-\sum_{j=0}^{v-1}\frac{\left(\lambda\beta(R^2-R_1^2)/2\right)^j}{j!}\exp\left(-\lambda\beta(R^2-R_1^2)/2\right).
\end{aligned}
$$

By substituting (73) into (54), the outage probability for Case I can be expressed as

$$
\begin{aligned}
&q_{\mathrm{out,f},v}^{\mathrm{I}} \\
&= \left(1-\widetilde{D}_T(K-1)\right)\mathbb{E}_{x_{\mathrm{f},v}}\left(1-\exp\left(-C_1 r_{\mathrm{f},v}^{\eta}\right)\right) \\
&= C_4\left(1-\int_{R_1}^{R}\exp\left(-C_1 r_{\mathrm{f},v}^{\eta}\right)C_3 r_{\mathrm{f},v}\left(r_{\mathrm{f},v}^2-R_1^2\right)^{v-1}\right. \\
&\qquad \left.\times\exp\left(-\beta\lambda r_{\mathrm{f},v}^2/2\right)\mathrm{d}r_{\mathrm{f},v}\right) \\
&\approx C_4\left(1-\frac{C_3(R-R_1)\pi}{2J}\sum_{j=1}^{J}\sqrt{1-\psi_j^2}\,r_{\mathrm{f},j}\right. \\
&\qquad \left.\times\left(r_{\mathrm{f},j}^2-R_1^2\right)^{v-1}\exp\left(-C_1 r_{\mathrm{f},j}^{\eta}-\frac{\beta\lambda}{2}r_{\mathrm{f},j}^2\right)\right). \qquad (74)
\end{aligned}
$$

The outage probability for Case II can be expressed as

$$
\begin{aligned}
&q_{\mathrm{out,f},v}^{\mathrm{II}} \\
&= \mathbb{E}_{x_{\mathrm{n},m},x_{\mathrm{f},v}}\left(\sum_{k=1}^{K-1}\mathbb{P}\left(\mathcal{D}=k\right)Q(k)\Big|N_{\mathrm{n}}\ge m,N_{\mathrm{f}}\ge v\right), (75)
\end{aligned}
$$

where $Q(k)$ is given in (61). By substituting the PDFs of $r_{\mathrm{n},m}$ and $r_{\mathrm{f},v}$ into (75), we obtain (76), shown at the top of the next page.

By following similar steps as for the proof of Proposition 1, we obtain

$$
q_{\mathrm{out,f},v}^{\mathrm{II}}
$$

$$q_{\text{out,f}}^{\text{II}} \approx \frac{4R_1^2}{R^2-R_1^2}\left(\sum_{k=k_{\min}+1}^{k_{\max}} \left(G(k-1)-G(k)\right)\int_0^{\frac{k}{K}R_{\text{f}}^{\text{th}}} G_2(z,k)G_3(z,k)A_4(z,k)\mathrm{d}z \right.$$
$$\left. + \int_0^{\frac{k}{K}R_{\text{f}}^{\text{th}}} G_2(z,k_{\min})G_3(z,k_{\min})\left(A_5(z,k_{\min})-G(k_{\min})A_4(z,k_{\min})\right)\mathrm{d}z\right), \tag{72}$$

$$q_{\text{out,f},v}^{\text{II}} = \frac{2}{\beta^2}C_2C_3\int_0^{R_1}\int_0^{\beta}\int_{R_1}^{R}\sum_{k=1}^{K-1}\left(\exp\left(-G(k)r_{\text{n},m}^{\eta}\right)-\exp\left(-G(k-1)r_{\text{n},m}^{\eta}\right)\right)$$
$$\times Q_z\left(r_{\text{f},v}, r_{\text{n},m}, \tau_D, k\right) r_{\text{f},v}^{\eta+1}\left(r_{\text{f},v}^2-R_1^2\right)^{v-1} r_{\text{n},m}^{2m-1}\exp\left(-\beta\lambda(r_{\text{f},v}^2+r_{\text{n},m}^2)/2\right)(\beta-\tau_D)\,\mathrm{d}r_{\text{f},m}\mathrm{d}\tau_D\mathrm{d}r_{\text{n},v}. \tag{76}$$

$$\approx \frac{R_1(R-R_1)C_2C_3}{4CLJ\beta}\sum_{c=1}^{C}\sqrt{1-\omega_c^2}\sum_{l=1}^{L}\sqrt{1-\zeta_l^2}$$
$$\times\left(\sum_{j=1}^{J}\sqrt{1-\psi_j^2}\sum_{k=1}^{K-1}Q_n(r_{\text{n},c},k)Q_z(r_{\text{f},j},r_{\text{n},c},\tau_{D,l},k)\right.$$
$$\times r_{\text{f},j}^{\eta+1}\left(r_{\text{f},j}^2-R_1^2\right)^{v-1} r_{\text{n},c}^{2m-1}(\beta-\tau_{D,l})$$
$$\left.\times\exp\left(-\beta\lambda\left(r_{\text{f},v}^2+r_{\text{n},m}^2\right)/2\right)\right). \tag{77}$$

Based on (74) and (77), we obtain (51). The proof of the proposition is complete.

References

[1] Y. Zhou, V. W.S. Wong, and R. Schober, "Performance analysis of cooperative NOMA with dynamic decode-and-forward relaying," in *Proc. of IEEE Globecom*, Singapore, Dec. 2017.

[2] L. Dai, B. Wang, Y. Yuan, S. Han, C.-L. I, and Z. Wang, "Non-orthogonal multiple access for 5G: Solutions, challenges, opportunities, and future research trends," *IEEE Commun. Mag.*, vol. 53, no. 9, pp. 74–81, Sept. 2015.

[3] M. Shirvanimoghaddam, M. Dohler, and S. Johnson, "Massive non-orthogonal multiple access for cellular IoT: Potentials and limitations," *IEEE Commun. Mag.*, vol. 55, no. 9, pp. 55–61, Sept. 2017.

[4] V. W.S. Wong, R. Schober, D.W.K. Ng, and L. C. Wang, *Key Technologies for 5G Wireless Systems*. Cambridge University Press, 2017.

[5] Y. Saito, A. Benjebbour, Y. Kishiyama, and T. Nakamura, "System-level performance evaluation of downlink non-orthogonal multiple access (NOMA)," in *Proc. of IEEE PIMRC*, London, UK, Sept. 2013.

[6] A. Benjebbovu, A. Li, Y. Saito, Y. Kishiyama, A. Harada, and T. Nakamura, "System-level performance of downlink NOMA for future LTE enhancements," in *Proc. of IEEE Globecom*, Atlanta, GA, Dec. 2013.

[7] J. Choi, "On the power allocation for MIMO-NOMA systems with layered transmissions," *IEEE Trans. Wireless Commun.*, vol. 15, no. 5, pp. 3226–3237, May 2016.

[8] Z. Wei, D. W. K. Ng, and J. Yuan, "Power-efficient resource allocation for MC-NOMA with statistical channel state information," in *Proc. of IEEE Globecom*, Washington, DC, Dec. 2016.

[9] Y. Sun, D. W. K. Ng, Z. Ding, and R. Schober, "Optimal joint power and subcarrier allocation for full-duplex multicarrier non-orthogonal multiple access systems," *IEEE Trans. Commun.*, vol. 65, no. 3, pp. 1077–1091, Mar. 2017.

[10] A. E. Mostafa, Y. Zhou, and V. W.S. Wong, "Connectivity maximization for narrowband IoT systems with NOMA," in *Proc. of IEEE ICC*, Paris, France, May 2017.

[11] Z. Ding, P. Fan, and H. V. Poor, "Impact of user pairing on 5G non-orthogonal multiple access downlink transmissions," *IEEE Trans. Veh. Technol.*, vol. 65, no. 8, pp. 6010–6023, Aug. 2016.

[12] Z. Ding, R. Schober, and H. V. Poor, "A general MIMO framework for NOMA downlink and uplink transmission based on signal alignment," *IEEE Trans. Wireless Commun.*, vol. 15, no. 6, pp. 4438–4454, Jun. 2016.

[13] Z. Ding, P. Fan, and H. V. Poor, "Random beamforming in millimeter-wave NOMA networks," *IEEE Access*, vol. 5, pp. 7667–7681, Feb. 2017.

[14] Z. Ding, X. Lei, G. K. Karagiannidis, R. Schober, J. Yuan, and V. K. Bhargava, "A survey on non-orthogonal multiple access for 5G networks: Research challenges and future trends," *IEEE J. Sel. Areas Commun.*, vol. 35, no. 10, pp. 2181–2195, Jul. 2017.

[15] Y. Zhou and V. W.S. Wong, "Stable throughput region of downlink NOMA transmissions with limited CSI," in *Proc. of IEEE ICC*, Paris, France, May 2017.

[16] Z. Ding, M. Peng, and H. V. Poor, "Cooperative non-orthogonal multiple access in 5G systems," *IEEE Commun. Lett.*, vol. 19, no. 8, pp. 1462–1465, Aug. 2015.

[17] Y. Liu, Z. Ding, M. Elkashlan, and H. V. Poor, "Cooperative non-orthogonal multiple access with simultaneous wireless information and power transfer," *IEEE J. Sel. Areas Commun.*, vol. 34, no. 4, pp. 938–953, Apr. 2016.

[18] J.-B. Kim and I.-H. Lee, "Non-orthogonal multiple access in coordinated direct and relay transmission," *IEEE Commun. Lett.*, vol. 19, no. 11, pp. 2037–2040, Nov. 2015.

[19] M. Xu, F. Ji, M. Wen, and W. Duan, "Novel receiver design for the cooperative relaying system with non-orthogonal multiple access," *IEEE Commun. Lett.*, vol. 20, no. 8, pp. 1679–1682, Aug. 2016.

[20] Z. Ding, H. Dai, and H. V. Poor, "Relay selection for cooperative NOMA," *IEEE Wireless Commun. Lett.*, vol. 5, no. 4, pp. 416–419, Aug. 2016.

[21] C. Zhong and Z. Zhang, "Non-orthogonal multiple access with cooperative full-duplex relaying," *IEEE Commun. Lett.*, vol. 20, no. 12, pp. 2478–2481, Dec. 2016.

[22] Z. Zhang, Z. Ma, M. Xiao, Z. Ding, and P. Fan, "Full-duplex device-to-device aided cooperative non-orthogonal multiple access," *IEEE Trans. Veh. Technol.*, vol. 66, no. 5, pp. 4467–4471, May 2017.

[23] K. Azarian, H. El Gamal, and P. Schniter, "On the achievable diversity-multiplexing tradeoff in half-duplex cooperative channels," *IEEE Trans. Inf. Theory*, vol. 51, no. 12, pp. 4152–4172, Dec. 2005.

[24] A. Murugan, K. Azarian, and H. El Gamal, "Cooperative lattice coding and decoding in half-duplex channels," *IEEE J. Sel. Areas Commun.*, vol. 25, no. 2, Feb. 2007.

[25] K. R. Kumar and G. Caire, "Coding and decoding for the dynamic decode and forward relay protocol," *IEEE Trans. Inf. Theory*, vol. 55, no. 7, pp. 3186–3205, Jul. 2009.

[26] M. Haenggi, *Stochastic Geometry for Wireless Networks*. Cambridge University Press, 2012.

[27] C. Zhai, W. Zhang, and G. Mao, "Cooperative spectrum sharing between cellular and ad-hoc networks," *IEEE Trans. Wireless Commun.*, vol. 13, no. 7, pp. 4025–4037, Jul. 2014.

[28] Y. Zhou and W. Zhuang, "Throughput analysis of cooperative communication in wireless ad hoc networks with frequency reuse," *IEEE Trans. Wireless Commun.*, vol. 14, no. 1, pp. 205–218, Jan. 2015.

[29] S. M. Alamouti, "A simple transmit diversity technique for wireless communications," *IEEE J. Sel. Areas Commun.*, vol. 16, no. 8, pp. 1451–1458, Oct. 1998.

[30] I. S. Gradshteyn and I. M. Ryzhik, *Table of Integrals, Series, and Products*. Academic Press, 2014.

[31] M. Abramowitz and I. A. Stegun, *Handbook of Mathematical Functions with Formulas, Graphs, and Mathematical Tables*. Dover Publications, 1972.

Yong Zhou (S'13, M'16) received the B.Sc. and M.Eng. degrees from Shandong University, Jinan, China, in 2008 and 2011, respectively, and the Ph.D. degree from the University of Waterloo, Waterloo, ON, Canada, in 2015. From 2015 to 2017, he worked as a postdoctoral research fellow in the Department of Electrical and Computer Engineering, The University of British Columbia, Vancouver, Canada. He is currently an Assistant Professor in the School of Information Science and Technology, ShanghaiTech University, China. His research interests include performance analysis and resource allocation of 5G networks. He has served as a technical program committee (TPC) member for several International conferences.

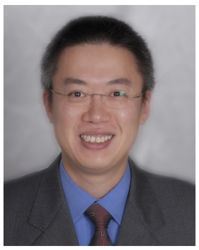

Vincent W.S. Wong (S'94, M'00, SM'07, F'16) received the B.Sc. degree from the University of Manitoba, Winnipeg, MB, Canada, in 1994, the M.A.Sc. degree from the University of Waterloo, Waterloo, ON, Canada, in 1996, and the Ph.D. degree from the University of British Columbia (UBC), Vancouver, BC, Canada, in 2000. From 2000 to 2001, he worked as a systems engineer at PMC-Sierra Inc. (now Microsemi). He joined the Department of Electrical and Computer Engineering at UBC in 2002 and is currently a Professor. His research areas include protocol design, optimization, and resource management of communication networks, with applications to wireless networks, smart grid, mobile cloud computing, and Internet of Things. Dr. Wong is an Editor of the *IEEE Transactions on Communications*. He has served as a Guest Editor of *IEEE Journal on Selected Areas in Communications* and *IEEE Wireless Communications*. He has also served on the editorial boards of *IEEE Transactions on Vehicular Technology* and *Journal of Communications and Networks*. He was a Technical Program Co-chair of *IEEE SmartGridComm*'14, as well as a Symposium Co-chair of *IEEE ICC*18, *IEEE SmartGridComm* ('13, '17) and *IEEE Globecom*'13. He is the Chair of the IEEE Vancouver Joint Communications Chapter and has served as a Chair of the IEEE Communications Society Emerging Technical Sub-Committee on Smart Grid Communications. He received the 2014 UBC Killam Faculty Research Fellowship.

Robert Schober (S'98, M'01, SM'08, F'10) received the Diplom (Univ.) and the Ph.D. degrees in electrical engineering from Friedrich-Alexander University of Erlangen-Nuremberg (FAU), Germany, in 1997 and 2000, respectively. From 2002 to 2011, he was a Professor and Canada Research Chair at the University of British Columbia (UBC), Vancouver, Canada. Since January 2012 he is an Alexander von Humboldt Professor and the Chair for Digital Communication at FAU. His research interests fall into the broad areas of Communication Theory, Wireless Communications, and Statistical Signal Processing.

Robert received several awards for his work including the 2002 Heinz MaierLeibnitz Award of the German Science Foundation (DFG), the 2004 Innovations Award of the Vodafone Foundation for Research in Mobile Communications, a 2006 UBC Killam Research Prize, a 2007 Wilhelm Friedrich Bessel Research Award of the Alexander von Humboldt Foundation, the 2008 Charles McDowell Award for Excellence in Research from UBC, a 2011 Alexander von Humboldt Professorship, a 2012 NSERC E.W.R. Stacie Fellowship, and a 2017 Wireless Communications Recognition Award by the IEEE Wireless Communications Technical Committee. He is listed as a 2017 Highly Cited Researcher by the Web of Science and a Distinguished Lecturer of the IEEE Communications Society (ComSoc). Robert is a Fellow of the Canadian Academy of Engineering and a Fellow of the Engineering Institute of Canada. From 2012 to 2015, he served as Editor-in-Chief of the IEEE Transactions on Communications. Currently, he is the Chair of the Steering Committee of the IEEE Transactions on Molecular, Biological and Multiscale Communication, a Member of the Editorial Board of the Proceedings of the IEEE, a Member at Large of the Board of Governors of ComSoc, and the ComSoc Director of Journals.